

1 **Weak population structure and expansive demographic history of the monogenean**
2 **parasite *Kapentagyrus* spp. infecting clupeid fishes of Lake Tanganyika**

3 **Nikol Kmentová^{1,2,3*}, Stephan Koblmüller⁴, Maarten Van Steenberge^{3,4,5,6}, Joost A.M.**
4 **Raeymaekers⁷, Tom Artois², Els L.R. De Keyzer^{3,8}, Leona Milec⁷, Fidel Muterezi Bukinga⁹, Théophile**
5 **Mulimbwa N'sibula⁹, Pascal Masilya Mulungula⁹, Gaspard Ntakimazi¹⁰, Filip A.M. Volckaert³,**
6 **Milan Gelnar¹, Maarten P.M. Vanhove^{1,2,3,11}**

7 ¹ Department of Botany and Zoology, Faculty of Science, Masaryk University, Kotlářská 2, 611 37
8 Brno, Czech Republic

9 ² Hasselt University, Centre for Environmental Sciences, Research Group Zoology: Biodiversity &
10 Toxicology, Agoralaan Gebouw D, B-3590 Diepenbeek, Belgium

11 ³ Laboratory of Biodiversity and Evolutionary Genomics, Department of Biology, University of
12 Leuven, Ch. Deberiotstraat 32, B-3000 Leuven, Belgium

13 ⁴ Institute of Biology, University of Graz, Universitätsplatz 2, A-8010 Graz, Austria

14 ⁵ Operational Directorate Taxonomy and Phylogeny, Royal Belgian Institute of Natural Sciences,
15 Vautierstraat 29, B-1000 Brussels, Belgium

16 ⁶ Biology Department, Royal Museum for Central Africa, Leuvensesteenweg 13, 3080, Tervuren,
17 Belgium

18 ⁷ Faculty of Biosciences and Aquaculture, Nord University, N-8049 Bodø, Norway

19 ⁸ Capacities for Biodiversity and Sustainable Development (CEBioS), Operational Directorate Natural
20 Environment, Royal Belgian Institute of Natural Sciences, Vautierstraat 29, B-1000, Brussels,
21 Belgium

22 ⁹ Centre de Recherche en Hydrobiologie, Département de Biologie, B.P. 73 Uvira, Democratic
23 Republic of Congo

24 ¹⁰ Département de Biologie, Université du Burundi, Campus Mutanga, B.P. 2700, Bujumbura,
25 Burundi

26 ¹¹ Zoology Unit, Finnish Museum of Natural History, University of Helsinki, P.O.Box 17, Helsinki FI-
27 00014, Finland

28 *corresponding author: kmentovan@mail.muni.cz, Laboratory of Parasitology, Department of
29 Botany and Zoology, Masaryk University, Kamenice 5, 625 00 Brno, Czech Republic

30 Note: Supplementary data associated with this article

31

32

33

34

35

36

37

38

39

40

41

42

43

44

45

46 **Abstract**

47 Lake Tanganyika is the oldest and deepest African Great Lake and harbours one of the most
48 diverse fish assemblages on earth. Two clupeid fishes, *Limnothrissa miodon* and *Stolothrissa*
49 *tanganicae*, constitute a major part of the total fish catch, making them indispensable for local
50 food security. Parasites have been proposed as indicators of stock structure in highly mobile
51 pelagic hosts. We examined the monogeneans *Kapentagyris limnothrissae* and *K. tanganicanus*
52 (Dactylogyridae) infecting these clupeids to explore the parasites' lake-wide population structure
53 and patterns of demographic history.

54 Samples were collected at seven sites distributed across three subbasins of the lake. Intraspecific
55 morphological variation of the monogeneans (N = 380) was analysed using morphometrics and
56 geomorphometrics of sclerotised structures. Genetic population structure of both parasite species
57 (N = 246) was assessed based on a 415 bp fragment of the mitochondrial COI gene.

58 Overall, we observed a lack of clear geographical morphological differentiation in both parasites
59 along a north-south axis. This lack of geographical population structure was also reflected by a
60 large proportion of shared haplotypes, and a pattern of seemingly unrestricted gene flow between
61 populations. Significant morphological and genetic differentiation between some populations
62 might reflect temporal differentiation rather than pure geographical isolation. Overall, the shallow
63 population structure of both species of *Kapentagyris* reflects the near-panmictic population
64 structure of both host species reported in previous studies. Morphological differences related to
65 host species identity of *K. tanganicanus* were consistent with incipient speciation observed at the
66 genetic level. Both parasite species experienced a recent demographic expansion, which might be
67 linked to paleohydrological events. Finally, hybridisation between species of *Kapentagyris* was
68 found, representing the first case in dactylogyrid monogeneans.

69 **Keywords:** Clupeidae, Dactylogyridae, Fisheries target species, *Kapentagyrus limnotrissae*,
70 *Kapentagyrus tanganicanus*, Phenotypic plasticity, Population genetics
71

72 **1. Introduction**

73 The pelagic realm of the African Great Lakes harbours a lower species diversity than the littoral
74 habitat. This might be attributed to the lower number of niches and a lack of barriers to gene flow
75 (Kirchberger et al., 2012; Shaw et al., 2000). Lake Tanganyika's pelagic zone is dominated by two
76 clupeid species (*Limnothrissa miodon* (Boulenger, 1906) and *Stolothrissa tanganicae* Regan, 1917)
77 and their latid fish predators. The two clupeids make up 65% (in mass) of the total catch in Lake
78 Tanganyika, making them a key component of the local fishery and an important factor for the
79 food security in the countries bordering the lake (Mölsä et al., 1999). Clupeids play an important
80 role in the food chain, because they are a link between the plankton and the piscivores (Coulter,
81 1991). Lake Tanganyika clupeids are parasitized by two species of *Kapentagyris* Kmentová, Gelnar
82 & Vanhove, 2018 (Monogenea, Dactylogyridae), *Kapentagyris limnotrissae* (Paperna, 1973) and
83 *Kapentagyris tanganicanus* Kmentová, Gelnar & Vanhove, 2018. Both parasite species have a
84 lake-wide distribution throughout the year (Kmentová et al., 2018). While *K. limnotrissae* is host
85 specific to *L. miodon*, *K. tanganicanus* has a more generalist lifestyle and infects both *L. miodon*
86 and *S. tanganicae*. In *K. tanganicanus*, two distinct morphotypes related to sardine species identity
87 have been observed (Kmentová et al., 2018).

88 Clupeids in Lake Tanganyika are short-lived species with a lifespan of usually one year and
89 maximally three years. Other biological characteristics include schooling behaviour and a diurnal
90 vertical migration that follows that of zooplankton (Coulter, 1991; Mulimbwa and Shirakihara,
91 1994). Migration and population connectivity of clupeids in the lake are poorly understood, but
92 are thought to be linked to seasonal changes in the plankton distribution (Kurki et al., 1999;
93 Plisnier et al., 2009). Generally, the delineation of pelagic fish stocks is crucial for fisheries
94 management (Emmett et al., 2005). Classical methods to track the movement of fish populations,
95 such as data storage tags (DST) and passive physical tags are no option for clupeids because of

96 their fragility (James et al., 1988). Hence, a combination of biological markers such as
97 morphometry, parasites, otolith elemental profiles, and molecular markers appears to be a more
98 promising approach (Svedäng et al., 2010). Lake-wide genome screening of both clupeids in Lake
99 Tanganyika using SNPs did not identify a clear population structure, suggesting near-panmictic
100 populations (De Keyzer et al., 2019; Junker et al., 2019). However, differences in chemical
101 composition of otoliths in both species (Sako et al., 2005) and a pattern of isolation by distance
102 along a north-south gradient in *S. tanganyicae* (De Keyzer et al., 2019) pointed to restricted long-
103 distance migration.

104 A combination of host- and parasite genetics has been proposed as an integrative approach to
105 reconstruct host population structure (Catalano et al., 2014) or stock structure over small
106 geographical and temporal scales (Baldwin et al., 2012). Monogenean parasites are excellent
107 targets for such research for several reasons. Foremost, the direct life cycle and often high host
108 specificity of monogeneans prevents their life history from being influenced by any other than the
109 targeted host taxon (Catalano et al., 2014; Pariselle et al., 2011). Secondly, due to their short
110 generation time, monogeneans may accumulate genetic changes more rapidly than their hosts
111 (Poulin, 2007). Thirdly, their high mutation rate in comparison to that of their hosts may reflect
112 historical events that are too recent to be inferred from host genetics (Nieberding et al., 2004;
113 Nieberding and Olivieri, 2007), and therefore parasites have been proposed to act as a
114 “magnifying glass” for their hosts. To date, few studies have used monogeneans in such an
115 approach. E.g., Pettersen et al. (2015) used a portion of the cytochrome c oxidase of *Gyrodactylus*
116 *thymalli* Žitňan, 1960 combined with dehydrogenase subunit 5 to indirectly infer barriers to gene
117 flow in grayling (*Thymallus thymallus* L.). Monogenean genetics was also used to track the
118 historical distribution of clariid catfishes in Africa (Barson et al., 2010) as well as to reconstruct
119 introduction pathways in *Perccottus glenii* Dybowski, 1877 (Ondračková et al., 2012).

120 Several steps have to be considered before using parasites as tags for host population structure,
121 including parasite species identification, the availability of more than one genetic marker to verify
122 cryptic species, and temporal stability in the presence of the parasite species across the host's
123 geographic range (Mattiucci et al., 2004; Vilas et al., 2005). All above-mentioned criteria are
124 fulfilled in the system studied here. Since the morphology of their sclerotised structures was
125 shown to vary along a north-south gradient (Kmentová et al., 2018), the species of *Kapentagyrus*
126 are proposed as candidates for unravelling the clupeids' population structure in Lake Tanganyika.
127 Moreover, several periods of draught in the past led to low lake levels and at times even
128 separation into up to four paleolakes corresponding with the current subbasins (Danley et al.,
129 2012; Sturmbauer et al., 2017). Such events repeatedly caused periods of population separation
130 followed by periods of secondary admixture across the north-south gradient. These left their
131 signature in the genetics of various animal taxa (Sturmbauer et al., 2001) and influenced their
132 current population structure (Nevado et al., 2013; Sefc et al., 2017; Sturmbauer et al., 2017), or
133 their demographic history, even in the barrier-free pelagic realm (Koblmüller et al., 2019). We
134 assume that the demographic history of *Kapentagyrus* spp. is connected with past population
135 trajectories of clupeid hosts, because historical lake level fluctuations influenced the demographic
136 history of cichlid fishes and their respective monogenean species in a similar way (Kmentová et al.,
137 2016; Koblmüller et al., 2019).

138 In this study, we test two species of *Kapentagyrus* as potential markers for spatio-temporal
139 population structure of both clupeid species. We hypothesise that there is more differentiation
140 among parasite populations than among host populations. We also compare the degree of
141 morphological and genetic differentiation among a host-specific versus a more generalist species
142 of *Kapentagyrus*. Finally, we test the relation between the hydrological history of Lake Tanganyika
143 and the recent demographic history of *Kapentagyrus* spp.

144 **2. Material and methods**

145 2.1. Sampling design

146 In total, 380 monogenean individuals collected from 497 host specimens were morphologically
147 analysed in this study. We used samples listed in Kmentová et al. (2018) as well as new specimens
148 collected in April 2018 (see Table 1). Monogeneans were collected from ethanol-preserved fish
149 samples collected along the lake's shoreline within two days in April 2018 (off Bujumbura,
150 Kalemie, Mpulungu and Uvira). As clupeids are highly mobile pelagic fish (De Keyzer et al., 2019;
151 Marshall, 1993; Mulimbwa and Mannini, 1993), this short time window enabled us to analyse the
152 spatial population structure of the parasites without the potential effect of school migration.
153 Additionally, fresh specimens collected within two days in August 2016 (off Kalemie and Uvira) and
154 within two weeks in Mpulungu 2018 were included in this study to analyse spatio-temporal
155 patterns in the parasites' morphology. We also included fresh specimens collected at Baraka in
156 2017, Mpulungu in 2016, Mvugo in 2016 and Mvuna Island in 2015 to increase spatial resolution
157 of population genetic analyses. In total, 246 individuals of *Kapentagyris* spp. were characterised
158 genetically (see Table 1).

159 All host specimens were either bought at fish markets in the above-mentioned cities or caught
160 with gills nets during experimental fishing. Fishes were identified to species level *in situ*. Voucher
161 specimens of the two clupeid species are part of the ichthyology collection of the Royal Museum
162 for Central Africa in Tervuren (RMCA 2016.20). Monogenean individuals collected from fresh fish
163 specimens were placed on a slide in a drop of glycerine ammonium picrate solution (GAP) in 1:1
164 ratio. Ethanol-preserved samples were cleaned of host tissue in a drop of water followed by
165 adding Hoyer's solution. In both cases, the individuals were fixed under a cover slip. All collected
166 monogenean species were identified as either *K. limnotrissae* or *K. tanganicus*. Infection
167 parameters are listed in Table 1. Voucher specimens of *Kapentagyris* spp. are deposited in the

168 collection of the Research Group Zoology: Biodiversity and Toxicology at Hasselt University in
169 Diepenbeek, Belgium (HU) (see Table 1 for accession numbers).

170 2.2. Morphometrics and geomorphometrics

171 Morphological variation on a lake wide geographical scale was inferred via both morphometric
172 and geomorphometric approaches. Haptoral and male copulatory hardparts of the two species of
173 *Kapentagyris* were measured and photographed using an Olympus BX51 microscope with
174 incorporated phase contrast at a magnification of 1000x (objective x100 immersion, ocular x10)
175 with *MicrolImage* v3.1. In total, we obtained 23 different morphometric parameters following the
176 terminology of Řehulková et al. (2013).

177 Geomorphometric data were obtained by digitising the shape of the dorsal and ventral anchor,
178 respectively. For this we used *tps Dig* v2.30 from the thin-plate spline (TPS) packages (Rohlf, 2006).
179 We chose the anchors for geomorphometric analyses as their shape had been successfully used in
180 intraspecific studies on members of *Ligophorus* Euzet & Suriano, 1977 (Monogenea,
181 Dactylogyridae) (Rodríguez-González et al., 2015). The shape of other monogeneans' sclerotised
182 structures, such as the shape of bars and marginal hooks, was shown to be highly related to the
183 method of sample preparation (Vignon et al., 2011). Eight fixed landmarks were selected on each
184 of the anchors. Additionally, semi-landmarks were placed in equal intervals on each anchor,
185 resulting in 98 of them in the case of *K. limnotrissae* and 102 in *K. tanganicus* (see Fig S1).

186 2.3. DNA extraction and genetic characterisation

187 Monogeneans were stored in 99% ethanol prior to DNA isolation. Subsequently, ethanol was
188 evaporated using a vacuum centrifuge and lysis buffer was poured onto the specimens. Whole
189 genomic DNA was extracted using either the Qiagen DNeasy Blood & Tissue Kit or Nucleospin

190 Tissue Genomic DNA kit following the manufacturer's instructions. The extracted DNA was eluted
191 in a volume of 50 µl.

192 Part of the monogenean mitochondrial cytochrome c oxidase subunit 1 (COI) gene was amplified
193 using a nested PCR reaction, in view of the low content of genomic DNA extracted from in most
194 cases 1/3 of the worm. The first PCR reaction was performed with ASmit1 (5'-
195 TTTTTTGGGCATCCTGAGGTTTAT-3') (Littlewood et al., 1997) and Schisto3 (5'-
196 TAATGCATMGGAAAAAACA-3') (Lockyer et al., 2003) primers in 24 µl of PCR mix (one unit of *Taq*
197 Polymerase, 1X buffer containing 2 mM MgCl₂, 0.2 mM dNTPs, 0.8 mM of each primer) for a total
198 reaction volume of 25 µl. It was carried out under the following conditions: initial denaturation at
199 95°C for 5 min, then 40 cycles of 1 min at 94°C, 1 min at 50°C and 1 min at 72°C, and final
200 elongation for 7 min at 72°C. The nested PCR with ASmit1 and ASmit2 (5'-
201 TAAAGAAAGAACATAATGAAAATG-3') (Littlewood et al., 1997) primers followed the same protocol
202 as the first one with 1:100 dilution of template DNA. The final PCR products were enzymatically
203 purified using 1 µl of ExoSAP-IT reagent and 2.5 µl of PCR product under the following conditions:
204 15 min at 37 °C and 15 min at 80 °C. The same primers as in the amplification reactions were used
205 for sequencing with a BigDye Terminator® Cycle Sequencing Kit v3.1 (ThermoFisher Scientific),
206 following the manufacturer's recommendations. The fragments were cleaned up using the BigDye
207 XTerminator® Purification Kit (ThermoFisher Scientific) and visualized on an ABI 3130 capillary
208 sequencer (Applied Biosystems).

209 For *S. tanganycae*, sequences of the mitochondrial cytochrome c oxidase subunit I (COI) gene were
210 obtained from De Keyzer et al. (2019) (GenBank accession numbers MH290064-159). For *L.*
211 *miodon*, DNA was extracted from finclips using the NucleoSpin Tissue kit (Macherey-Nagel GmbH)
212 according to the manufacturer's instructions. Subsequently, the COI gene was amplified using the
213 universal primer combination HCO2198 (5'-TAAACTTCAGGGTGACCAAAAATCA-3') and LCO1490
214 (5'-GGTCAACAAATCATAAAGATATTGG-3') (Folmer et al., 1994). PCR reaction was performed in 24

215 μl of PCR mix (12.5 μl MyTaq HS mix (2x) (Bioline, London, UK), 10.5 μl H₂O and 1 μl primer mix
216 (20 μM of each primer) to which 1 μl of purified DNA was added for a total reaction volume of 25
217 μl (Handy et al., 2011). It was carried out under the following conditions: initial denaturation at
218 94°C for 3 min, then 35 cycles of 45 sec at 94°C, 40 sec min at 52°C and 90 sec at 72°C, and final
219 elongation for 10 min at 72°C. PCR products were purified using CleanPCR beads (CleanNA, GC
220 Biotech). The same primers as in the amplification reactions were used for sequencing with a
221 BigDye Terminator® Cycle Sequencing Kit v3.1 (ThermoFisher Scientific), following the
222 manufacturer's recommendations. The fragments were purified CleanDTR beads (CleanNA, GC
223 Biotech) and visualized on an ABI 3500XL capillary sequencer (Applied Biosystems).
224 DNA sequences were visually inspected and corrected using MEGA v7 (Kumar et al., 2016) and
225 aligned using MUSCLE (Edgar, 2004) under default distance measures as implemented in MEGA.
226 COI sequences of *Kapentagyris* spp. are deposited in NCBI GenBank under the accession numbers
227 MK598125-323. Corresponding nuclear data generated by Kmentová et al. (2018) are available on
228 NCBI GenBank under the accession numbers MH071782 and MH071808 (28S, 18S and ITS-1 region
229 of *K. limnotrissae*), MH071783 and MH071807 (28S, 18S and ITS-1 region of *K. tanganicus*
230 collected from *L. miodon*), MK522517-520 (28S, 18S and ITS-1 region of *K. tanganicus* collected
231 from *Stolothrissa tanganicæ*), MK521656-MK521659 (28S rDNA portion of *K. limnotrissae*
232 individuals identified as hybrids) and MK521661-MK521664 (18S and ITS-1 rDNA portion of *K.*
233 *limnotrissae* individuals identified as hybrids). COI sequences of *L. miodon* are deposited in NCBI
234 GenBank under the accession numbers MT040511-78. Individuals of both host species originate
235 from different localities covering all three major subbasins of Lake Tanganyika (see Table S1).

236

237 2.4. Data analysis

238

239 2.4.1. Morphological differentiation

240 To avoid any possible influence of ethanol fixation on the size and shape of sclerotised structures,
241 the samples were subdivided into spatial (ethanol-preserved) and spatio-temporal (fresh) data
242 sets. To evaluate intraspecific and intrahost variation, data sets were further subdivided into six
243 different sample sets according to parasite species and host species. These sample sets were
244 always analysed separately by a) morphometric analyses of haptoral structures, and
245 geomorphometric analyses of b) dorsal and c) ventral anchors. Samples in all sample sets and
246 subsequent analyses were grouped by sampling site to check for possible geographical structure in
247 both species of *Kapentagyris*. As preliminary analyses indicated a significant influence of host size
248 on morphological characters, individuals of *K. tanganicus* ex *L. miodon* from Kalemie 2018 were
249 analysed as two groups using 12 cm of host standard length (SL) as a cut off value (referred to as
250 Kalemie 2018 Big and Kalemie 2018 Small, respectively). As the same pattern was discovered with
251 the fresh samples from Mpulungu, a threshold in SL of host specimens was set to 10 cm (referred
252 to as Mpulungu 2018 Big and Mpulungu 2018 Small, respectively).

253 *Morphometrics* - Principal component analysis (PCA) of haptoral morphometric parameters
254 standardised to unit scale was performed in the R package *ade4* (Jombart, 2008). Missing data
255 were replaced by the average value for each morphological character. To increase the resolution
256 of the resulting pattern, morphological characters with more than 50% missing data were
257 excluded prior to the analysis. Then, linear or generalised linear models were calculated in the R
258 package *stats* (R Core Team, 2013) to evaluate the effect of sampling site, host size and their
259 interaction on each of the morphological characters followed by F-statistic and Chi Square
260 statistics, respectively. In case of an overall significant effect of sampling site, *post hoc* Welch's t
261 test and Tukey test, respectively, were performed to assess pairwise significance between
262 sampling sites. Sampling sites with insufficient number of specimens (< 10) were excluded from
263 the analyses.

264 *Geomorphometrics* - Configurations of fixed landmarks were superimposed using Generalized Full
265 Procrustes Analyses (Cox and Cox, 1989; Zelditch et al., 2012), under the Least Squares criterion to
266 minimize bending energy with respect to a mean reference shape. Canonical variate analyses
267 (CVA) (Klingenberg and Monteiro, 2005) and PCA using only the fixed landmarks were performed
268 in *MorphoJ* v2.0 (Klingenberg, 2011). A permutation test with 10,000 iterations was used to
269 statistically validate pairwise differences between the pre-defined groups. Additionally, the overall
270 shape of both anchors, captured using fixed landmarks and semi-landmarks, was analysed using
271 *tpsRelw* v1.49. A Relative Warp Analysis (RWA) (Rohlf, 1993) was performed with the Procrustes
272 coordinates. The scaling option was set to $\alpha = 0$ to give all landmarks equal weight. Sampling sites
273 with insufficient number of specimens (<6 as in the case of *K. tanganicanus* ex *L. miodon* from
274 Bujumbura 2018 and *K. tanganicanus* ex *S. tanganiccae* from Bujumbura 2018 and Mpulungu 2018
275 in spatial sample sets) were excluded from the analyses.

276 Relationships between the individual scores inferred with PCA and RWA analyses, respectively,
277 and the host size were checked via linear regression analyses in the R package *stats* (R Core Team,
278 2013). This was done for each sample set and within the respective groups. All sample sets were
279 visually inspected for outliers, which were excluded from the analyses. Normality of the data was
280 checked by Shapiro-Wilks tests in the R package *onewaytests* (Dag et al., 2018). The homogeneity
281 of variance among groups within each sample set was assessed by Levene's tests in the R package
282 *car* (Fox and Weisberg, 2011). Biplots of PC and RW scores were visualised with the packages
283 *ggplot2* (Wickham, 2009) and *factoextra* (Kassambara and Mundt, 2017).

284 2.4.2. Genetic structure

285 The genetic diversity of the two monogenean species and the two host species was studied based
286 on 415 bp (*Kapentagyryus* spp.), 646 bp (*L. miodon*) and 643 bp (*S. tanganiccae*), respectively, of the
287 COI gene. Genetic diversity was assessed as the number of haplotypes and polymorphic sites,

288 haplotype diversity and nucleotide diversity, all calculated using *Arlequin* v3.5 (Excoffier and
289 Lischer, 2010).

290 The genealogy of the COI haplotypes for the parasites were inferred by means of a Median Joining
291 network in *PopART* v1.71 (Leigh and Bryant, 2015). Differentiation among pre-defined populations
292 was estimated by F_{ST} in *Arlequin* v3.5 (Excoffier and Lischer, 2010): for *K. tanganicanus* collected
293 from *L. miodon* and *S. tanganicæ*, respectively, in Uvira 2016, as well as for populations of *K.*
294 *tanganicanus* ex *L. miodon* with at least 17 individuals available. Analysis of molecular variance
295 (AMOVA) based on F-statistics was used to test for significant population structure of *K.*
296 *tanganicanus* at the level of subbasins within Lake Tanganyika. Sample size for *K. limnotrissae* was
297 generally too low to allow for any meaningful population genetic analyses.

298 2.4.3. Demographic history

299 To test for signals of past population expansion in both species of monogeneans and their host
300 species, two different neutrality test statistics, Tajima's D (Tajima, 1989) and Fu's F_s (Fu, 1997),
301 were calculated in *Arlequin* v3.5 (Excoffier and Lischer, 2010).

302 The demographic history of *Kapentagyryus* spp. was further assessed by mismatch distribution
303 analyses in *Arlequin* v3.5 (Excoffier and Lischer, 2010). The sum of square deviations (SSD) and
304 raggedness index (rg) were used to assess the fit of the observed mismatch distributions to the
305 expectations based on estimates of the growth parameter. Past population size trajectories of
306 monogenean species were further investigated with a Bayesian skyline plot (Drummond et al.,
307 2005), as implemented in *BEAST* v1.8.2. (Suchard et al., 2018). The substitution rate was set to
308 10% per million years, which is lower than the rates previously used for viviparous gyrodactylid
309 monogenean species characterised by asexual multiplication (Meinilä et al., 2004), and should
310 take into account the assumed comparatively longer generation time and lower reproductive
311 capacity of *Kapentagyryus* as oviparous dactylogyrid monogeneans (Tinsley, 2004). Two

312 independent MCMC runs of 300 million generations each and a sampling frequency of 30,000
313 were conducted, with a burn-in of the first 10% of sampled generations. The number of grouped
314 intervals was set to 5. Verification of effective sample sizes (ESS > 200 for all parameters), tracing
315 MCMC runs and visualisation of past population size changes were done in *Tracer* v1.7 (Rambaut
316 et al., 2018).

317 **3. Results**

318 3.1. Morphological variation

319 3.1.1. *Kapentagyryus limnotrissae* ex *Limnothrissa miodon*

320 Overall, the intraspecific morphological variation of *K. limnotrissae* was primarily affected by
321 several parameters of the dorsal anchor, ventral anchor and branch length of the ventral bar (Fig.
322 1B, Table S2). An overview of measurements from haptoral as well as from the male copulatory
323 organ region is listed in Table S4.

324 *Haptoral structures* - PCA did not reveal any clear geographical separation based on haptoral
325 morphometric parameters in *K. limnotrissae* along any of the PC axes in any of the two sample sets
326 (Fig. 2A&B). However, differentiation was visible between the specimens from Mpulungu 2018
327 and Uvira 2016 along the first and the second axis (Fig. 2B). In half of the comparisons between
328 sampling sites tested, at least one of the morphological parameters was found to differ
329 significantly. The length of the outer root of the ventral anchor was the only morphological
330 character that differed between sampling sites in both sample sets (see Fig. 1 and Table S2).

331 *Dorsal and ventral anchor* - In *K. limnotrissae*, the PCA biplot based on fixed landmarks revealed a
332 clearer differentiation between Uvira and Bujumbura 2018 for the dorsal than for the ventral
333 anchor (Fig. 2C and Fig. S2A). This differentiation was further reflected in the CVA results (Table
334 S3). The shape of the ventral anchor was significantly different between the specimens from Uvira

335 and Kalemie 2016, and between Kalemie 2016 and Mpulungu 2018 (detailed results presented in
336 Table S2). The results of RWA (including sliding landmarks) confirmed the pattern obtained via PCA
337 (Fig. S2).

338 *Effect of host size* - No effect of host size on the position of specimens in neither of the presented
339 biplots was detected (not shown). Linear models for the spatial sample set revealed that the total
340 length of the dorsal anchor decreased with host size ($F_{1,58} = 5.32$, $P < 0.05$). This was also the case
341 for the point length of the dorsal anchor ($\chi^2_{2,57} = 9.98$, $P = 0.002$) in the spatio-temporal sample set.
342 Linear models revealed an increasing effect of host size on the branch length of the dorsal bar
343 ($F_{2,60} = 9.17$, $P < 0.05$) and the inner root length of the ventral anchor ($\chi^2_{2,61} = 5.34$, $P = 0.02$) in the
344 spatio-temporal sample set.

345 3.1.2. *Kapentagyris tanganicanus* ex *Limnothrissa miodon*

346 Overall, the intraspecific morphological variation in *K. tanganicanus* ex *L. miodon* was affected by
347 several parameters of both the dorsal and the ventral anchor, the dorsal and the ventral bar as
348 well as some of the pairs of marginal hooks (Fig. 1C, Table S2). An overview of measurements from
349 the haptoral as well as the male copulatory organ region are given in Table S5.

350 *Haptoral structures* - The first PC axis of haptoral morphometric parameters revealed that
351 specimens from Mpulungu 2018 were intermediate between those from Kalemie 2018 and Uvira
352 2018 (Fig 3A). The separation was further reflected in the number of significantly different
353 characters between the sampling sites (see Table S2). A separation was also visible along the first
354 PC axis of haptoral morphometric parameters between specimens collected in Mpulungu 2018
355 from those from Kalemie 2016 and Uvira 2016 (Fig. 3B). Only two morphological parameters
356 differed significantly between Mpulungu 2018 and Uvira 2016 (see Table S2). A single one differed
357 significantly between the two host-size categories from Kalemie 2018 and Mpulungu 2018.

358 *Dorsal and ventral anchor* - In *K. tanganicanus* ex *L. miodon*, the PCAs of the shape of both
359 anchors, based on a fixed landmark geomorphometric approach, reflected the gradient visible in
360 the biplot of the haptoral morphometric approach in the both spatial and the spatio-temporal
361 sample sets (Fig. 3C-F). This differentiation was further supported by the CVA results. Here, a
362 significant difference was observed in at least one of the anchors in comparisons between each of
363 the sampling sites. The only exception was the comparison between Mpulungu 2018 and Uvira
364 2018, where no difference was found (see also Table S3). Moreover, the shape of the ventral
365 anchor and of both anchors differed significantly between the two host-size categories from
366 Kalemie 2018 and Mpulungu 2018, respectively. The results of RWA (including sliding landmarks)
367 confirmed the pattern obtained via PCA (Fig. S3).

368 *Effect of host size* - A significant effect of host size was detected only on the individual RW scores
369 of the first axis for the ventral anchor of the spatio-temporal sample set ($F_{1,64} = 7.08$, $P = 0.010$).
370 Linear models revealed an increasing effect of host size on the total length of the ventral anchor
371 ($F_{3,77} = 34.31$, $P < 0.0010$) and the length to notch of the ventral anchor ($\chi^2_{3,77} = 10.81$, $P = 0.001$) in
372 the case of spatio-temporal sample set.

373 3.1.3 *Kapentagyris tanganicanus* ex *Stolothrissa tanganicae*

374 Overall, the intraspecific morphological variation of *K. tanganicanus* ex *S. tanganicae* was affected
375 by the length to notch of the dorsal anchor and the second pair of marginal hooks (Fig. 1D, Table
376 S2). An overview of measurements from the haptoral as well as from the male copulatory organ
377 region is listed in Table S6.

378 *Haptoral structures* - In total, two sample sets, both containing specimens of *K. tanganicanus* ex *S.*
379 *tanganicae* from four and two different groups, respectively, were analysed. Clear differentiation
380 was visible in the second PC axis of haptoral morphometric parameters between the specimens
381 from Kalemie 2018 and Uvira 2018 (Fig. 4A). A single morphological character, the size of the first

382 pair of marginal hooks, differed significantly between sampling sites. Additionally, a separation in
383 the spatio-temporal sample set was found between specimens from Mpulungu 2018 and Uvira
384 2016 along the first and second PC axes (Fig. 4B). Similar to the previous sample set, only one
385 morphological character, the length to the notch of the dorsal anchor, differed between sampling
386 sites.

387 *Dorsal and ventral anchor* - The position of specimens along the first PC axis of the anchor shape
388 based on a fixed landmark geomorphometric approach mirrored the pattern observed in haptoral
389 morphometric characters in both sample sets (Fig. 4C-F). In the spatial sample set, the shape of
390 ventral anchor was found to be related to the sampling site in the comparison between Kalemie
391 2018 and Uvira 2018. In the spatio-temporal sample set, the shape of botch anchors was different
392 between Mpulungu 2018 and Uvira 2016 (Table S3). The results of RWA (including sliding
393 landmarks) followed the pattern (Fig. S4).

394 *Effect of host size* - No effect of the host size on the position of specimens was detected in neither
395 of the presented biplots nor in the linear models for the morphological parameters.

396 In total, just a single morphological character, the length to notch of the dorsal anchor, differed
397 between the sampling sites in all sample sets. Two additional characters, the branch length of the
398 ventral bar and the total length of the ventral anchor, differed between the sampling sites in
399 specimens of *Kapentagyris* spp. collected from *L. miodon*. Finally, the length of the first pair of
400 marginal hooks differed between the sampling sites for the specimens of *K. tanganicanus*
401 collected from different host species (see 3.1.2.). For further details see Table S2.

402 3.2. Genetic diversity

403 The number of polymorphic sites in COI found per monogenean species was 18 (N = 51) for *K.*
404 *limnotrissae* and 68 (N = 140) for *K. tanganicanus*. Both clupeids had a similar number of

405 polymorphic sites, 45 (N = 69) in *L. miodon* and 48 (N = 96) in *S. tanganyicae*, in the COI gene.
406 Similar levels of nucleotide and haplotype diversity were observed between the two parasite
407 species and one of the host species: *S. tanganyicae*. Lower genetic diversity was observed for *K.*
408 *tanganyicanus* when only individuals collected from *S. tanganyicae* were included. The other host
409 species, *L. miodon*, had higher genetic diversity than both species of *Kapentagyryus* (Table 2).

410 3.3. Parasite population genetics

411 First, there was no evident clustering of *K. tanganyicanus* according to host species (see Fig. 5A).
412 However, significant F_{ST} value were found between *K. tanganyicanus* infecting different host
413 species collected in Uvira 2016 ($F_{ST} = 0.0668$; $P = 0.0112$). Haplotype networks indicated neither
414 geographic, nor school-related structure in either of the monogenean species. All networks
415 showed a star-like topology with a single dominant haplotype (see Fig. 5B-D). Satellite haplotypes
416 were mostly separated by a single mutation from the central haplotypes. Significant F_{ST} values
417 were also recorded in *K. tanganyicanus* ex *L. miodon* between several sampling sites on a temporal
418 scale (see enclosed table in Fig. 5). AMOVA calculated for *K. tanganyicanus* ex *L. miodon* showed
419 that most of the variation was present within populations (96.85%) in comparison to 1.67% among
420 populations within subbasins and 1.47% among subbasins.

421 3.4. Demographic history

422 Signatures of population expansion were detected in both monogenean species and their host
423 species. Recent population growth was suggested by significantly negative values of Fu's F_s in *K.*
424 *limnotrissae* (-20.98; $P < 0.001$), in *K. tanganyicanus* (-27.90; $P < 0.001$), in *L. miodon* (24.09; $P <$
425 0.001) and in *S. tanganyicae* (-61.64; $P < 0.001$) as well as Tajima's D in *K. limnotrissae* (-2.48; $P <$
426 0.001), in *K. tanganyicanus* (-2.41; $P < 0.001$) and in *S. tanganyicae* (-2.41; $P < 0.001$). In *L. miodon*,
427 the value of Tajima's D was negative (-1.31) but not significant ($P = 0.06$).

428 The unimodal mismatch distribution was well supported by a non-significant SSD and rg , indicating
429 recent population expansion in both *Kapentagyris* species (see Fig. 6A, B). Mismatch analyses
430 dated the onset of population expansion to 11.8 KYA in *K. limnotrissae* (95% CI: 6.5–16.8 KYA) and
431 to 17.6 KYA in *K. tanganicanus* (95% CI: 3.3–30.1 KYA).

432 Based on Bayesian Skyline Plot analysis, the start of population growth for *K. tanganicanus* was
433 estimated around 12 KYA (see Fig. 6D) and the time to the most recent common ancestor (TMRCA)
434 around 70.9 KYA (95% HDP: 15.6–143.1 KYA). Due to the insufficient number of haplotypes, BSP
435 could not track past changes of effective population size back to more than 7 KYA in the case of *K.*
436 *limnotrissae* (see Fig. 6C). No sign of population growth was observed and the TMRCA was
437 estimated at 14.4 KYA (95% HDP: 6.5–24.1 KYA).

438 3.5. Nuclear-mitochondrial discordance

439 Based on the comparison of rDNA markers published in Kmentová et al. (2018) and the obtained
440 COI sequences of the same specimens, nuclear–mitochondrial discordance was documented for
441 four individuals of *Kapentagyris* collected from *L. miodon* (see Fig. 5A). For two of these four
442 cases, morphological vouchers are available (specimens on slides deposited under X.4.04 and
443 XI.1.20 in HU). Their morphology and haplotype of 28S and/or 18S and ITS-1 rDNA (MK521656–59
444 and MK521661–64) are characteristic for *K. limnotrissae*, whereas the mitochondrial COI
445 haplotype is that of *K. tanganicanus*.

446 Discussion

447 The geographic and temporal population structure, and demographic history of two monogenean
448 species of *Kapentagyris* infecting clupeid hosts in Lake Tanganyika were investigated. Although,
449 morphological comparison of the parasites' sclerotised structures did not show clear patterns of
450 differentiation along a north-south axis, significant differences between some of them indicate

451 spatio-temporal differentiation. Moreover, molecular analyses suggest a weak geographic
452 population structure with some temporal differentiation. Finally, both species of *Kapentagyris*
453 showed a similar pattern of recent population expansion, presumably correlated with Pleistocene
454 climate change and subsequent lake-level fluctuations.

455 *Monogeneans as tags for the geographical population structure of clupeids*

456 The pelagic environment, promoting dispersal, and the large effective population size constrain
457 genetic drift and differentiation in pelagic fishes (Gonzalez and Zardoya, 2007; Koblmüller et al.,
458 2019; Martínez et al., 2006). Moreover, the patchy production of phytoplankton in Lake
459 Tanganyika may promote seasonal migration following the prey and population mixing in pelagic
460 fishes (Phiri and Shirakihara, 1999; Plisnier et al., 2009; van Zwieten et al., 2002). On the other
461 hand, population differentiation in the pelagic realm might be facilitated by the presence of
462 physical barriers such as currents (Podsetchine and Huttula, 2000) or geographical distance
463 (Gonzalez and Zardoya, 2007). Although the migration patterns of clupeids have not been resolved
464 yet, some isolation by distance along a north-south gradient was detected, suggesting limits to
465 lake-wide migration in *S. tanganyicae* (De Keyzer et al., 2019). This was also seen in the chemical
466 composition of otoliths in both species (Sako et al., 2005).

467 *Morphological variation* - Based on our comprehensive study, morphometrics of monogenean
468 haptoral and male copulatory organ structures showed in some cases significant intraspecific
469 shape variation with respect to sampling site. However, none of the approaches used identified a
470 morphological character that was unambiguously specific to a particular sampling site in neither of
471 the various sample sets. Interestingly, even though the shape of both anchors mirrored the
472 pattern of the overall haptoral morphology, the detailed morphology of neither of these
473 structures provided sufficient resolution to resolve the geographic origin of a monogenean
474 individual. Significantly different morphological characters between the sampling sites in 2016

475 were not found between the specimens from the same localities in 2018. This suggests
476 dependency of phenotypic differentiation on environmental conditions rather than fidelity to a
477 geographic location in *Kapentagyryus* spp. and consequently of their clupeid host species.
478 Temperature (Brazenor et al., 2018; Dávidová et al., 2005; Ergens and Gelnar, 1985; Mo, 1993),
479 pollutants (Beaumont, 1997) or other environmental factors (Cable and Harris, 2002; Olstad et al.,
480 2009) influence the morphology of monogeneans. The morphological differences of *Kapentagyryus*
481 spp. observed between some of the sampling sites might hence be attributed to environmental
482 factors directly influencing the parasites' morphology or indirectly through host morphology.
483 These may induce geographical patterns via restricted host - parasite migration, or via similar
484 environmental conditions in geographically isolated locations. This might explain the clustering of
485 geographically isolated specimens of *K. tanganicanus* from Mpulungu and Kalemie (Fig. 3A).
486 Interestingly, spatio-temporal variation in sample sets of fresh supported the hypothesis of
487 environmentally-dependent variation, specific to site and time. In Lake Tanganyika, geographical
488 and seasonal variation in thermal stratification, the level of oxygen (Hecky et al., 1978; Langenberg
489 et al., 2002), pH (Plisnier et al., 1999), chemical (Degens et al., 1971), phytoplankton composition
490 (Descy et al., 2005) and algal succession (Agawin et al., 2000) have been reported. They are driven
491 mostly by wind conditions (Hecky et al., 1978; Langenberg et al., 2003). However, no experimental
492 data for representatives of *Kapentagyryus* are currently available to attribute observed
493 morphological differentiation to specific environmental factor.

494 *Different host, different story* - Interestingly, the number of morphometric characters related to
495 sampling site differed between the sample sets. While a maximum of two characters was
496 informative in the case of *K. limnotrissae*, a species specific to *L. miodon*, this number was
497 considerably higher in *K. tanganicanus* collected from the same host species. Clupeids form size-
498 dependent schools (Misund, 1993). Host-size dependent intensity of infection between

499 *Kapentagyris* spp. collected from *L. miodon* was observed (*K. limnotrissae* being more prevalent
500 on smaller *L. miodon* and vice versa, own unpublished results). Therefore, observed discrepancy in
501 differentiation between species of *Kapentagyris* might be explained by a difference in migration
502 capacity between fish schools (Nøttestad et al., 1999). Moreover, the number of significantly
503 different morphological characters between the groups of *K. tanganicus* ex *S. tanganicus* was
504 lower compared to the individuals collected from *L. miodon*. Such a pattern might be related to
505 the difference in ecology between the host species as *S. tanganicus* displays more pelagic life style
506 compared to *L. miodon* (Mannini et al., 1996; Mulimbwa and Mannini, 1993). However, this result
507 might also be influenced by the small number of specimens collected from *S. tanganicus*.

508 *Genetic population structure* - Generally, the genetic structure of parasites is strongly connected
509 with the dispersal capacity of their hosts (Miura et al., 2006) and their reproductive mode,
510 generation time and population size. The COI-based median joining networks of both monogenean
511 species exhibited comparable core-satellite topologies with similar levels of variation in haplotype
512 and nucleotide diversity. Given that no clear geographical structure appeared from the haplotype
513 network of none of the three monogenean/host species combinations, we suggest geographical
514 panmixia with temporal effects in both species of monogeneans infecting Lake Tanganyika
515 clupeids. This result corresponds with the general biology of clupeids, with assumed lake-wide
516 migration patterns (De Keyzer et al., 2019; Hauser et al., 1998; Junker et al., 2019; Mulimbwa and
517 Shirakihara, 1994). In general, studies conducted on marine clupeids do not show strong
518 population structure, neither using genetic markers (García-Rodríguez et al., 2011; Gonzalez and
519 Zardoya, 2007; Kinsey et al., 1994) nor fish tags (Clark, 1945). Nevertheless, and despite the shared
520 COI haplotypes, significant genetic divergence among some of the pre-defined populations of *K.*
521 *tanganicus* from *L. miodon* was detected based on F_{ST} . Such temporal genetic structure without
522 clear evidence for a geographical pattern could be explained by restricted migration of clupeid

523 hosts, random genetic drift across generations or cohorts related to overfishing of declining
524 clupeid populations in the lake (Mölsä et al., 1999) or recruitment-dependent population
525 fluctuations in r-strategic fish stocks (Watanabe et al., 1995). Interestingly, a recent study by
526 Junker et al. (2019) suggested that population structure in *L. miodon* is linked to chromosomal
527 inversions. Notably, genetic diversity of *K. tanganicanus* in COI is comparable to its host: *S.*
528 *tanganicae*. However, when only parasite individuals collected from this host species were
529 included, the value was lower. Nucleotide diversity in *L. miodon* is much higher than in both
530 species of *Kapentagyris* (see Table 2). The level of genetic variation and impact of genetic drift
531 depends on effective population size (Nei and Tajima, 1981). Given the observed variability in
532 prevalence and infection intensity of *Kapentagyris* spp. (see Table 1), it is hard to estimate
533 population size relative to their clupeid hosts and subsequently evaluate the effect of host
534 population fluctuations. However, no temporal differentiation was observed in neither of the
535 clupeid hosts so far (De Keyzer et al., 2019; Junker et al., 2019). The reported genetic divergence
536 of *K. tanganicanus* among pre-defined geographical populations can be influenced by stochasticity
537 related to the small sample size and short fragment length rather than persisting gene flow
538 barriers. Moreover, the generally reported short generation time of less than a month in
539 dactylogyrid monogeneans (Harris, 1983; Scott and Nokes, 1984; Xiaoqin et al., 2000). Indeed,
540 multiple spawning events per year were reported for both species of Tanganyika clupeids
541 (Mulimbwa and Shirakihara, 1994). Together with their short life span, this may erase the
542 expected effect of a faster molecular evolution in parasites. Alternatively, monogean
543 reproduction in the pelagic habitat connected with planktonic larval dispersal might cause
544 differences in local genetic diversity of parasites. This is known as fluctuating genetic patchiness
545 (Hellberg et al., 2002). A similar mechanism was suggested for populations of several monogean
546 species infecting pelagic fish hosts along the coast of China (Li et al., 2011; Shi et al., 2014; Wang
547 et al., 2016; Yan et al., 2016).

548 We need to know more about the population dynamics of the hosts and parasites to identify the
549 cause of the mosaic population structure revealed in this study. In order to further evaluate the
550 magnifying potential of *Kapentagyris* spp., genome-wide markers need to be applied and
551 compared with similar data on the host species as this study is limited by the single genetic marker
552 being used. A promising approach to clarify the true nature of the interaction between
553 environment, host and parasite are waterscape genomic and transcriptomic studies (Grummer et
554 al., 2019). Here, the peculiarities of the aquatic environment are taken in consideration in the
555 analysis of populations. Promising examples are the highly resolved population structure of well-
556 dispersing taxa (Clucas et al., 2018) and dual transcriptomic studies in host and parasite (Feis et al.,
557 2018).

558 *Parasite diversification in the pelagic zone of Lake Tanganyika*

559 The core-satellite structure of the haplotype networks and the lower haplotype and nucleotide
560 diversity in comparison to *Cichlidogyrus casuarinus* Pariselle, Muterezi Bukinga & Vanhove, 2015, a
561 monogenean species infecting bathybatine benthopelagic cichlids in Lake Tanganyika (Kmentová
562 et al., 2016; Pariselle et al., 2015) points to more recent diversification in both species of
563 *Kapentagyris*. This might be attributed to limited allopatric divergence in view of a higher
564 dispersal capacity and larger population densities of clupeids in Lake Tanganyika compared to
565 pelagic cichlid species (Coulter, 1991; Koblmüller et al., 2019, 2015).

566 Interestingly, morphological differentiation of *K. tanganicanus*, influenced by the host species and
567 detected in a previous study (Kmentová et al., 2018), was supported by genetic differentiation of
568 the specimens sampled off Uvira in 2016. Our results indicate genetic differentiation of *K.*
569 *tanganicanus* with respect to the clupeid host species. Most probably it happened after a recent
570 host switch. However, given the uniformity in three nuclear gene fragments, the low F_{ST} value and
571 the many shared COI haplotypes of *K. tanganicanus* collected from different host species, we

572 hypothesize that speciation is prevented as hosts occupy the same environment and have a prey-
573 predator relationship between them (Coulter, 1991; Mulimbwa and Shirakihara, 1994), which has
574 been proposed to be linked to host sharing in monogeneans (Strona, 2015). This should be further
575 verified by genetic characterisation of more individuals combined with genome wide data. The
576 results fit the scenario of a relatively low rate of intraspecific divergence in barrier-free pelagic
577 compared to littoral fish species (Kmentová et al., 2016; Koblmüller et al., 2019, 2015).

578 *Demographic history*

579 Haplotype structure pointed to a recent population expansion for both species of *Kapentagyryus*
580 and their clupeid hosts. The time of the onset of population growth inferred for *K. tanganicanus*
581 corresponded with global climate changes and subsequent lake level rise. Indeed, 10 KYA is the
582 estimated end of the last Little Ice Age, which corresponds with the end of a dry period in East
583 Africa (McGlue et al., 2008). Sea level changes and climate oscillations have measurably influenced
584 the demographic history of monogeneans (Wang et al., 2016; Yan et al., 2016). We suggest that
585 expansion and population growth of *Kapentagyryus* spp. are linked to rising lake levels. We assume
586 that such patterns might be also found in the clupeid host species as climate induced lake level
587 fluctuations have also influenced the demographic history of eupelagic bathybatine cichlids
588 (Koblmüller et al., 2019) and their monogenean parasite *C. casuarinus* (Kmentová et al., 2016). The
589 onset of population expansion and the time to the most recent common ancestor was estimated
590 for both species of *Kapentagyryus* to have been more recent than for *C. casuarinus* (using the same
591 substitution rate). Possible explanations for this difference could be the different life-style and
592 population size of the hosts, host range of the parasites and difference in substitution rates.

593 *Nuclear–mitochondrial discordance*

594 The mitochondrial haplotype of *K. tanganicanus* was detected in four specimens identified as *K.*
595 *limnotrissae*. We interpret this as evidence for mitochondrial introgression of *K. tanganicanus* into

596 *K. limnotrissae*. All four individuals were homozygous at all three nuclear loci analysed and
597 identical to other individuals of *K. limnotrissae*, which excludes that they are F1 hybrids of
598 *Kapentagyryus* spp. Given the broader host range of *K. tanganicanus* compared to its congener, the
599 introgression might result from a recent host switch and a demographic expansion of *K.*
600 *tanganicanus* (Barson et al., 2010; Rieseberg et al., 2007; Seixas et al., 2018). However, our data
601 does not allow unambiguous differentiation among incomplete lineage sorting, introgression, or
602 contemporary hybridisation. Nevertheless, as no intermediate nuclear haplotype was captured,
603 the presence of a mitochondrial genome of one species in the nuclear environment of another
604 species suggests mitochondrial introgression followed by recurrent backcrossing into the paternal
605 species. Eventually, the introgression resulted in dilution and loss of alleles inherited from the
606 maternal species (Okamoto et al., 2010). A hybridisation event would support the above-
607 mentioned scenario of a recent host switch of *K. tanganicanus* followed by temporal
608 differentiation of infection related to host size (own unpublished data). Moreover, the apparent
609 morphological similarity in the male copulatory organ of the two parasite species contradicts the
610 scenario of intrahost speciation (Jarkovský et al., 2004). Although hybridisation has been reported
611 in gyrodactylid monogeneans (Barson et al., 2010; Schelkle et al., 2012), this is the first case for
612 dactylogyrid monogeneans. The poor documentation of hybridisation in monogeneans might be
613 related to the lack of studies combining morphology, nuclear and mitochondrial markers. In
614 general, hybridisation is considered a major driver of evolution (Franssen et al., 2015; Hedrick,
615 2013; Huyse et al., 2013; King et al., 2015) which also impacts the host range of parasites (Henrich
616 et al., 2013; Huyse et al., 2009).

617 *Conclusion*

618 In conclusion, no consistent geographical structure along a north-south axis in neither
619 *Kapentagyryus* spp. was found (distance between the two most extreme sampling sites is > 600

620 km), suggesting ongoing gene flow throughout Lake Tanganyika. Therefore, our results correspond
621 with a pattern of weak to no lake-wide population structure of both host species (De Keyzer et al.,
622 2019; Junker et al., 2019). Temporal structure in some morphological characters might be
623 attributed to similar environmental conditions in geographically isolated sampling sites, in
624 combination with restricted host migration. Moreover, significant genetic differentiation was
625 found between some of the parasite populations. Serial sampling and genomic data should
626 increase spatio-temporal resolution to track host migration. Some evidence for incipient
627 speciation in *K. tanganicus* according to host species was found based on mitochondrial data,
628 despite uniformity in nuclear gene portions. Our findings provide additional support for the impact
629 of historical lake level changes also on organisms inhabiting the lake's pelagic zone. Finally,
630 mitonuclear discordance suggests past hybridisation between the two species of *Kapentagyryus*,
631 which is the first documented case of hybridisation in dactylogyrid monogeneans.

632 **Acknowledgments**

633 The authors would like to thank to L. Raisingerová, C. Rahmouni, H. Zimmermann, A. P. H. Bose
634 and W. Salzburger for help with collecting host samples. M. Jorissen is gratefully acknowledged for
635 fruitful discussions about monogenean morphological variability and help in the lab. Special thanks
636 to the staff of the parasitological group at Masaryk University, Brno (Czech Republic), the Research
637 Group Zoology at Hasselt University (Belgium), Research Centre of Hydrobiology in Uvira (DR
638 Congo) and Fisheries Research Unit in Mpulungu (Zambia) for their hospitality.

639 **Funding**

640 Research has been supported by the Czech Science Foundation (P505/12/G112 (ECIP) and GA19-
641 13573S), EMBRC Belgium - FWO project GOH3817N as well as by a joint program between the
642 Austrian agency for international mobility and cooperation in education, science and research and
643 the Ministry of Education, Youth and Sports (project number 8J18AT007), the Austrian Agency for

644 International Cooperation in Education and Research (OEAD; project number CZ 08/2018; to SK).
645 MPMV was co-financed by institutional funding of the Finnish Museum of Natural History and the
646 Belgian Directorate-General for Development Cooperation and Humanitarian Aid (CEBioS
647 program). ELRDk was supported by the Belgian Development Cooperation through VLIR-UOS
648 (VLADOC scholarship NDOC2016PR006 to ELRDk and South Initiative project CD2018SIN218A101).
649 Fieldwork was carried out with the approval of the competent local authorities under mission
650 statement 031/MINRST/CRH-U/2016 and the permission of the Fisheries Department of Zambia
651 and under a study permit issued by the government of Zambia (SP 008732).

652

653 **References**

- 654 Agawin, N.S.R., Duarte, C.M., Agustí, S., 2000. Nutrient and temperature control of the
655 contribution of picoplankton to phytoplankton biomass and production. *Limnol. Oceanogr.*
656 45, 591–600. <https://doi.org/10.4319/lo.2000.45.3.0591>
- 657 Baldwin, R.E., Banks, M.A., Jacobson, K.C., 2012. Integrating fish and parasite data as a holistic
658 solution for identifying the elusive stock structure of Pacific sardines (*Sardinops sagax*). *Rev.*
659 *Fish Biol. Fish.* 22, 137–156. <https://doi.org/10.1007/s11160-011-9227-5>
- 660 Barson, M., Přikrylová, I., Vanhove, M.P.M., Huyse, T., 2010. Parasite hybridization in African
661 *Macrogyrodactylus* spp. (Monogenea, Platyhelminthes) signals historical host distribution.
662 *Parasitology* 137, 1585–1595. <https://doi.org/10.1017/S0031182010000302>
- 663 Beaumont, M., 1997. Book review: Sublethal and chronic effects of pollutants on freshwater fish,
664 edited by R. Müller and R. Lloyd. *Regul. Rivers Res. Manag.* 13, 95–96.
665 [https://doi.org/10.1002/\(SICI\)1099-1646\(199701\)13:1<95::AID-RRR428>3.0.CO;2-V](https://doi.org/10.1002/(SICI)1099-1646(199701)13:1<95::AID-RRR428>3.0.CO;2-V)
- 666 Brazenor, A.K., Saunders, R.J., Miller, T.L., Hutson, K.S., 2018. Morphological variation in the

667 cosmopolitan fish parasite *Neobenedenia girellae* (Capsalidae: Monogenea). Int. J. Parasitol.
668 48, 125–134. <https://doi.org/10.1016/J.IJPARA.2017.07.009>

669 Cable, J., Harris, P.D., 2002. Gyrodactylid developmental biology: historical review, current status
670 and future trends. Int. J. Parasitol. 32, 255–80.

671 Catalano, S.R., Whittington, I.D., Donnellan, S.C., Gillanders, B.M., 2014. Parasites as biological tags
672 to assess host population structure: Guidelines, recent genetic advances and comments on a
673 holistic approach. Int. J. Parasitol. Parasites Wildl. 3, 220–6.
674 <https://doi.org/10.1016/j.ijppaw.2013.11.001>

675 Clark, F.N., 1945. Results of tagging experiments in California on Sardine (*Sardinops caerulea*). Fish.
676 Bull. 61, 93.

677 Clucas, G. V., Younger, J.L., Kao, D., Emmerson, L., Southwell, C., Wienecke, B., Rogers, A.D., Bost,
678 C.A., Miller, G.D., Polito, M.J., Lelliott, P., Handley, J., Crofts, S., Phillips, R.A., Dunn, M.J.,
679 Miller, K.J., Hart, T., 2018. Comparative population genomics reveals key barriers to dispersal
680 in Southern Ocean penguins. Mol. Ecol. 27, 4680–4697. <https://doi.org/10.1111/mec.14896>

681 Coulter, G.W., 1991. Pelagic Fish, in: Coulter, G.W. (Ed.), Lake Tanganyika and Its Life. Natural
682 History Museum & Oxford University Press, London Oxford & New York, pp. 111–150.

683 Cox, C.F., Cox, M.A.A., 1989. Procrustes analysis, in: Cox, C.F., Cox, M.A.A. (Eds.), Multidimensional
684 Scaling. Second Edition. Chapman & Hall, London, pp. 123–139.
685 <https://doi.org/10.1137/1028043>

686 Dag, O., Dolgun, A., Konar, N.M., 2018. onewaytests: an R package for one-way tests in
687 independent groups designs. R J. 10, 175–199. <https://doi.org/doi.org/10.32614/RJ-2018-022>

688 Danley, P.D., Husemann, M., Ding, B., Dipietro, L.M., Beverly, E.J., Peppe, D.J., 2012. The impact of

689 the geologic history and paleoclimate on the diversification of East African cichlids. *Int. J. Evol.*
690 *Biol.* 574851. <https://doi.org/10.1155/2012/574851>

691 Dávidová, M., Jarkovský, J., Matějusková, I., Gelnar, M., 2005. Seasonal occurrence and metrical
692 variability of *Gyrodactylus rhodei* Žitňan 1964 (Monogenea, Gyrodactylidae). *Parasitol. Res.*
693 95, 398–405. <https://doi.org/10.1007/s00436-005-1311-0>

694 De Keyzer, E.L.R., De Corte, Z., Van Steenberge, M., Raeymaekers, J.A.M., Calboli, F.C.F.,
695 Kmentová, N., N'Sibula Mulimbwa, T., Virgilio, M., Vangestel, C., Mulungula, P.M., Volckaert,
696 F.A.M., Vanhove, M.P.M., 2019. First genomic study on Lake Tanganyika sprat *Stolothrissa*
697 *tanganicae*: a lack of population structure calls for integrated management of this important
698 fisheries target species. *BMC Evol. Biol.* 19, 6. <https://doi.org/10.1186/s12862-018-1325-8>

699 Degens, E.T., Von Herzen, R.P., Wong, H.-K., 1971. Lake Tanganyika: Water chemistry, sediments,
700 geological structure. *Naturwissenschaften* 58, 229–241. <https://doi.org/10.1007/BF00602986>

701 Descy, J.P., Hardy, M.A., Sténuite, S., Pirlot, S., Leporcq, B., Kimirei, I., Sekadende, B., Mwaitega,
702 S.R., Sinyenza, D., 2005. Phytoplankton pigments and community composition in Lake
703 Tanganyika. *Freshw. Biol.* 50, 668–684. <https://doi.org/10.1111/j.1365-2427.2005.01358.x>

704 Drummond, A.J., Rambaut, A., Shapiro, B., Pybus, O.G., 2005. Bayesian coalescent inference of
705 past population dynamics from molecular sequences. *Mol. Biol. Evol.* 22, 1185–1192.
706 <https://doi.org/10.1093/molbev/msi103>

707 Edgar, R.C., 2004. MUSCLE: Multiple sequence alignment with high accuracy and high throughput.
708 *Nucleic Acids Res.* 32, 1792–1797. <https://doi.org/10.1093/nar/gkh340>

709 Emmett, R.L., Brodeur, R.D., Miller, T.D., Pool, S.S., Krutzikowsky, G.K., Bentley, P.J., Mccrae, J.,
710 2005. Pacific sardine (*Sardinops sagax*) abundance, distribution, and ecological relationships
711 in the Pacific Northwest. *Calif. Coop. Ocean. Fish. Investig. Rep.* 46, 122–143.

712 Ergens, R., Gelnar, M., 1985. Experimental verification of the effect of temperature on the size of
713 the hard parts of haptor of *Gyrodactylus katharineri* Malberg 1964. *Folia Parasitol. (Praha)*.
714 32, 377–380.

715 Excoffier, L., Lischer, H.E.L., 2010. Arlequin suite ver 3.5: a new series of programs to perform
716 population genetics analyses under Linux and Windows. *Mol. Ecol. Resour.* 10, 564–567.
717 <https://doi.org/10.1111/j.1755-0998.2010.02847.x>

718 Feis, M.E., John, U., Lokmer, A., Luttikhuisen, P.C., Wegner, K.M., 2018. Dual transcriptomics
719 reveals co-evolutionary mechanisms of intestinal parasite infections in blue mussels *Mytilus*
720 *edulis*. *Mol. Ecol.* 27, 1505–1519. <https://doi.org/10.1111/mec.14541>

721 Folmer, O., Black, M., Hoeh, W., Lutz, R., Vrijenhoek, R., 1994. DNA primers for amplification of
722 mitochondrial cytochrome c oxidase subunit I from diverse metazoan invertebrates. *Mol.*
723 *Mar. Biol. Biotechnol.* 3, 294–299. <https://doi.org/10.1071/ZO9660275>

724 Fox, J., Weisberg, S., 2011. An {R} companion to applied regression, Second. ed. Sage, Thousand
725 Oaks {CA}.

726 Franssen, F., Bilska-Zajac, E., Deksné, G., Sprong, H., Pozio, E., Rosenthal, B., Rozycki, M., van der
727 Giessen, J., 2015. Genetic evidence of interspecies introgression of mitochondrial genomes
728 between *Trichinella spiralis* and *Trichinella britovi* under natural conditions. *Infect. Genet.*
729 *Evol.* 36, 323–332. <https://doi.org/10.1016/J.MEEGID.2015.10.005>

730 Fu, Y.X., 1997. Statistical tests of neutrality of mutations against population growth, hitchhiking
731 and background selection. *Genetics* 147, 915–25.

732 García-Rodríguez, F.J., García-Gasca, S.A., Cruz-Agüero, J.D. La, Cota-Gómez, V.M., 2011. A study of
733 the population structure of the Pacific sardine *Sardinops sagax* (Jenyns, 1842) in Mexico
734 based on morphometric and genetic analyses. *Fish. Res.* 107, 169–176.

735 <https://doi.org/10.1016/J.FISHRES.2010.11.002>

736 Gonzalez, E.G., Zardoya, R., 2007. Relative role of life-history traits and historical factors in shaping
737 genetic population structure of sardines (*Sardina pilchardus*). BMC Evol. Biol. 7, 197.
738 <https://doi.org/10.1186/1471-2148-7-197>

739 Grummer, J.A., Beheregaray, L.B., Bernatchez, L., Hand, B.K., Luikart, G., Narum, S.R., Taylor, E.B.,
740 2019. Aquatic landscape genomics and environmental effects on genetic variation. Trends
741 Ecol. Evol. <https://doi.org/10.1016/j.tree.2019.02.013>

742 Handy, S.M., Deeds, J.R., Ivanova, N. V., Hebert, P.D.N., Hanner, R.H., Ormos, A., Weigt, L.A.,
743 Moore, M.M., Yancy, H.F., 2011. A single-laboratory validated method for the generation of
744 DNA barcodes for the identification of fish for regulatory compliance. J. AOAC Int. 94, 201–
745 210.

746 Harris, P.D., 1983. The morphology and life-cycle of the oviparous *Oögyrodactylus farlowellae* gen.
747 et sp.nov. (Monogenea, Gyrodactylidea). Parasitology 87, 405–420.
748 <https://doi.org/10.1017/S0031182000082937>

749 Hauser, L., Carvalho, G.R., Pitcher, T.J., 1998. Genetic population structure in the Lake Tanganyika
750 sardine *Limnothrissa miodon*. J. Fish Biol. 53, 413–429. [https://doi.org/10.1111/j.1095-](https://doi.org/10.1111/j.1095-8649.1998.tb01040.x)
751 [8649.1998.tb01040.x](https://doi.org/10.1111/j.1095-8649.1998.tb01040.x)

752 Hecky, R.E., Fee, E.J., Kling, H., Rudd, J.W.M., 1978. Studies on the planktonic ecology of Lake
753 Tanganyika. Winnipeg, Man.: Fisheries and Marine Service.

754 Hedrick, P.W., 2013. Adaptive introgression in animals: examples and comparison to new mutation
755 and standing variation as sources of adaptive variation. Mol. Ecol. 22, 4606–4618.
756 <https://doi.org/10.1111/mec.12415>

757 Hellberg, M.E., Burton, R.S., Neigel, J.E., Palumbi, S.R., 2002. Genetic assessment of connectivity
758 among marine populations. *Bull. Mar. Sci.* 70, 273–290.

759 Henrich, T., Benesh, D.P., Kalbe, M., 2013. Hybridization between two cestode species and its
760 consequences for intermediate host range. *Parasit. Vectors* 6, 33.
761 <https://doi.org/10.1186/1756-3305-6-33>

762 Huyse, T., Van den Broeck, F., Hellemans, B., Volckaert, F.A.M., Polman, K., 2013. Hybridisation
763 between the two major African schistosome species of humans. *Int. J. Parasitol.* 43, 687–689.
764 <https://doi.org/10.1016/J.IJPARA.2013.04.001>

765 Huyse, T., Webster, B.L., Geldof, S., Stothard, J.R., Diaw, O.T., Polman, K., Rollinson, D., 2009.
766 Bidirectional introgressive hybridization between a cattle and human schistosome species.
767 *PLoS Pathog.* 5, e1000571. <https://doi.org/10.1371/journal.ppat.1000571>

768 James, A.G., Hutchings, L., Brownell, C.L., Horstman, D.A., 1988. Methods of capture and transfer
769 to the laboratory of wild pelagic fish. *South African J. Mar. Sci.* 6, 17–21.
770 <https://doi.org/10.2989/025776188784480519>

771 Jarkovský, J., Morand, S., Šimková, A., Gelnar, M., 2004. Reproductive barriers between congeneric
772 monogenean parasites (*Dactylogyus*: Monogenea): Attachment apparatus morphology or
773 copulatory organ incompatibility? *Parasitol. Res.* 92, 95–105.
774 <https://doi.org/10.1007/s00436-003-0993-4>

775 Jombart, T., 2008. Adegnet: A R package for the multivariate analysis of genetic markers.
776 *Bioinformatics* 24, 1403–1405. <https://doi.org/10.1093/bioinformatics/btn129>

777 Junker, J., Rick, J.A., McIntyre, P.B., Kimirei, I., Sweke, E.A., Mosille, J.B., Werli, B., Dinkel, C.,
778 Mwaiko, S., Seehausen, O., Wagner, C.E., 2019. Sex differentiation and a chromosomal
779 inversion lead to cryptic diversity in Lake Tanganyika sardines. *bioRxiv* 800904.

780 <https://doi.org/10.1101/800904>

781 Kassambara, A., Mundt, F., 2017. factoextra: extract and visualize the results of multivariate data
782 analyses.

783 King, K.C., Stelkens, R.B., Webster, J.P., Smith, D.F., Brockhurst, M.A., 2015. Hybridization in
784 parasites: consequences for adaptive evolution, pathogenesis, and public health in a changing
785 w. PLOS Pathog. 11, e1005098. <https://doi.org/10.1371/journal.ppat.1005098>

786 Kinsey, S.T., Orsoy, T., Bert, T.M., Mahmoudi, B., 1994. Population structure of the Spanish sardine
787 *Sardinella aurita*: natural morphological variation in a genetically homogeneous population.
788 Mar. Biol. 118, 309–317. <https://doi.org/10.1007/BF00349798>

789 Kirchberger, P.C., Sefc, K.M., Sturmbauer, C., Koblmüller, S., 2012. Evolutionary history of Lake
790 Tanganyika's predatory deepwater cichlids. Int. J. Evol. Biol. 2012, 716209,
791 [10.1155/2012/716209](https://doi.org/10.1155/2012/716209). <https://doi.org/10.1155/2012/716209>

792 Klingenberg, C.P., 2011. MORPHOJ: an integrated software package for geometric morphometrics.
793 Mol. Ecol. Resour. 11, 353–357. <https://doi.org/10.1111/j.1755-0998.2010.02924.x>

794 Klingenberg, C.P., Monteiro, L.R., 2005. Distances and directions in multidimensional shape spaces:
795 implications for morphometric applications. Syst. Biol. 54, 678–688.
796 <https://doi.org/10.1080/10635150590947258>

797 Kmentová, N., Gelnar, M., Mendlová, M., Van Steenberge, M., Koblmüller, S., Vanhove, M.P.M.,
798 2016. Reduced host-specificity in a parasite infecting non-littoral Lake Tanganyika cichlids
799 evidenced by intraspecific morphological and genetic diversity. Sci. Rep. 6, 39605.
800 <https://doi.org/10.1038/srep39605>

801 Kmentová, N., Van Steenberge, M., Raeymaekers, J.A.R., Koblmüller, S., Hablützel, P.I., Muterezi

802 Bukinga, F., Mulimbwa N'sibula, T., Masilya Mulungula, P., Nzigidahera, B., Ntakimazi, G.,
803 Gelnar, M., Vanhove, M.P.M., 2018. Monogenean parasites of sardines in Lake Tanganyika:
804 diversity, origin and intra-specific variability. *Contrib. to Zool.* 87, 105–132.

805 Koblmüller, S., Odhiambo, E.A., Sinyinza, D., Sturmbauer, C., Sefc, K.M., 2015. Big fish, little
806 divergence: phylogeography of Lake Tanganyika's giant cichlid, *Boulengerochromis microlepis*.
807 *Hydrobiologia* 748, 29–38. <https://doi.org/10.1007/s10750-014-1863-z>

808 Koblmüller, S., Zangl, L., Börger, C., Daill, D., Vanhove, M.P.M., Sturmbauer, C., Sefc, K.M., 2019.
809 Only true pelagics mix: comparative phylogeography of deepwater bathybatine cichlids from
810 Lake Tanganyika. *Hydrobiologia* 832, 93–103. <https://doi.org/10.1007/s10750-018-3752-3>

811 Kumar, S., Stecher, G., Tamura, K., Gerken, J., Pruesse, E., Quast, C., Schweer, T., Peplies, J.,
812 Ludwig, W., Glockner, F., 2016. MEGA7: Molecular evolutionary genetics analysis Version 7.0
813 for bigger datasets. *Mol. Biol. Evol.* 33, 1870–1874. <https://doi.org/10.1093/molbev/msw054>

814 Kurki, H., Vuorinen, I., Bosma, E., Bwebwa, D., 1999. Spatial and temporal changes in copepod
815 zooplankton communities of Lake Tanganyika, in: Lindqvist, O. V., Molsd, H., Salonen, K.,
816 Sarvala, J. (Eds.), *From Limnology to Fisheries: Lake Tanganyika and Other Large Lakes*. Kluwer
817 Academic Publishers., Dordrecht, pp. 105–114. [https://doi.org/10.1007/978-94-017-1622-](https://doi.org/10.1007/978-94-017-1622-2_10)
818 [2_10](https://doi.org/10.1007/978-94-017-1622-2_10)

819 Langenberg, V.T., Mwape, L.M., Tshibangu, K., Tumba, J.-M., Koelmans, A.A., Roijackers, R.,
820 Salonen, K., Sarvala, J., Mölsä, H., 2002. Comparison of thermal stratification, light
821 attenuation, and chlorophyll- a dynamics between the ends of Lake Tanganyika. *Aquat.*
822 *Ecosyst. Health Manag.* 5, 255–265. <https://doi.org/10.1080/14634980290031956>

823 Langenberg, V.T., Sarvala, J., Roijackers, R., 2003. Effect of wind induced water movements on
824 nutrients, chlorophyll- a, and primary production in Lake Tanganyika. *Aquat. Ecosyst. Health*

825 Manag. 6, 279–288. <https://doi.org/10.1080/14634980301488>

826 Leigh, J.W., Bryant, D., 2015. PopART: full-feature software for haplotype network construction.
827 Methods Ecol. Evol. 6, 1110–1116.

828 Li, M., Shi, S.F., Brown, C.L., Yang, T.B., 2011. Phylogeographical pattern of *Mazocraeoides*
829 *gonialosae* (Monogenea, Mazocraeidae) on the dotted gizzard shad, *Konosirus punctatus*,
830 along the coast of China. Int. J. Parasitol. 41, 1263–1272.
831 <https://doi.org/10.1016/j.ijpara.2011.07.012>

832 Littlewood, D.T.J., Rohde, K., Clough, K.A., 1997. Parasite speciation within or between host
833 species? - Phylogenetic evidence from site-specific polystome monogeneans. Int. J. Parasitol.
834 27, 1289–1297. [https://doi.org/10.1016/S0020-7519\(97\)00086-6](https://doi.org/10.1016/S0020-7519(97)00086-6)

835 Lockyer, A.E., Olson, P.D., Ostergaard, P., Rollinson, D., Johnston, D.A., Attwood, S.W., Southgate,
836 V.R., Horak, P., Snyder, S.D., Le, T.H., Agatsuma, T., McManus, D.P., Carmichael, A.C., Naem,
837 S., Littlewood, D.T.J., 2003. The phylogeny of the Schistosomatidae based on three genes with
838 emphasis on the interrelationships of *Schistosoma* Weinland, 1858. Parasitology 126, 203–24.
839 <https://doi.org/https://doi.org/10.1017/S0031182002002792>

840 Mannini, P., Aro, E., Katonda, K.I., Kassaka, B., Mambona, C., Milindi, G., Paffen, P., Verburg, P.,
841 1996. Pelagic fish stocks of Lake Tanganyika: biology and exploitation. FAO/FINNIDA research
842 for the management of the fisheries of Lake Tanganyika., GCP/RAF/271/FIN—TD/53 (En).
843 Bujumbura.

844 Marshall, B.E., 1993. Biology of the African clupeid *Limnothrissa miodon* with reference to its small
845 size in artificial lakes. Rev. Fish Biol. Fish. 3, 17–38. <https://doi.org/10.1007/BF00043296>

846 Martínez, P., González, E.G., Castilho, R., Zardoya, R., 2006. Genetic diversity and historical
847 demography of Atlantic bigeye tuna (*Thunnus obesus*). Mol. Phylogenet. Evol. 39, 404–416.

848 <https://doi.org/10.1016/j.ympev.2005.07.022>

849 Mattiucci, S., Abaunza, P., Ramadori, L., Nascetti, G., 2004. Genetic identification of *Anisakis* larvae
850 in European hake from Atlantic and Mediterranean waters for stock recognition. *J. Fish Biol.*
851 65, 495–510. <https://doi.org/10.1111/j.0022-1112.2004.00465.x>

852 McGlue, M.M., Lezzar, K.E., Cohen, A.S., Russell, J.M., Tiercelin, J.-J., Felton, A.A., Mbede, E.,
853 Nkotagu, H.H., 2008. Seismic records of late Pleistocene aridity in Lake Tanganyika, tropical
854 East Africa. *J. Paleolimnol.* 40, 635–653. <https://doi.org/10.1007/s10933-007-9187-x>

855 Meinilä, M., Kuusela, J., Ziętara, M.S., Lumme, J., 2004. Initial steps of speciation by geographic
856 isolation and host switch in salmonid pathogen *Gyrodactylus salaris* (Monogenea:
857 Gyrodactylidae). *Int. J. Parasitol.* 34, 515–526. <https://doi.org/10.1016/j.ijpara.2003.12.002>

858 Misund, O., 1993. Dynamics of moving masses: variability in packing density, shape, and size
859 among herring, sprat, and saithe schools. *ICES J. Mar. Sci.* 50, 145–160.
860 <https://doi.org/10.1006/jmsc.1993.1016>

861 Miura, O., Torchin, M.E., Kuris, A.M., Hechinger, R.F., Chiba, S., 2006. Introduced cryptic species of
862 parasites exhibit different invasion pathways. *Proc. Natl. Acad. Sci. U. S. A.* 103, 19818–23.
863 <https://doi.org/10.1073/pnas.0609603103>

864 Mo, A., 1993. Seasonal variation of haptor hard parts of *Gyrodactylus derjavini* Mikailov 1975
865 (Monogenea: Gyrodactylidae) on brown trout *Salmo trutta* L. parr and Atlantic salmon *Salmo*
866 *salar* L. parr in the River Sandviksela, N. *Syst. Parasitol.* 26, 225–231.

867 Mölsä, H., Reynolds, J.E., Coenen, E.J., Lindqvist, O.V., 1999. Fisheries research towards resource
868 management on Lake Tanganyika. *Hydrobiologia* 407, 1–24.
869 <https://doi.org/10.1023/A:1003712708969>

870 Mulimbwa, N., Mannini, P., 1993. Demographic characteristics of *Stolothrissa tanganyicae*,
871 *Limnothrissa miodon* and *Lates stappersii* in the Northwestern (Zairean) waters of Lake
872 Tanganyika. CIFA Occas. Pap.

873 Mulimbwa, N., Shirakihara, K., 1994. Growth, recruitment and reproduction of sardines
874 (*Stolothrissa tanganyicae* and *Limnothrissa miodon*) in northwestern Lake Tanganyika. Tropics
875 4, 57–67. <https://doi.org/10.3759/tropics.4.57>

876 Nei, M., Tajima, F., 1981. Genetic drift and estimation of effective population size. Genetics 98,
877 625–640.

878 Nevado, B., Mautner, S., Sturmbauer, C., Verheyen, E., 2013. Water-level fluctuations and
879 metapopulation dynamics as drivers of genetic diversity in populations of three Tanganyikan
880 cichlid fish species. Mol. Ecol. 22, 3933–3948. <https://doi.org/10.1111/mec.12374>

881 Nieberding, C., Morand, S., Libois, R., Michaux, J.R., 2004. A parasite reveals cryptic
882 phylogeographic history of its host. Proceedings. Biol. Sci. 271, 2559–68.
883 <https://doi.org/10.1098/rspb.2004.2930>

884 Nieberding, C.M., Olivieri, I., 2007. Parasites: proxies for host genealogy and ecology? Trends Ecol.
885 Evol. 22, 156–165. <https://doi.org/10.1016/j.tree.2006.11.012>

886 Nøttestad, L., Giske, J., Holst, J.C., Huse, G., 1999. A length-based hypothesis for feeding
887 migrations in pelagic fish. Can. J. Fish. Aquat. Sci. 56, 26–34. <https://doi.org/10.1139/f99-222>

888 Okamoto, M., Nakao, M., Blair, D., Anantaphruti, M.T., Waikagul, J., Ito, A., 2010. Evidence of
889 hybridization between *Taenia saginata* and *Taenia asiatica*. Parasitol. Int. 59, 70–74.
890 <https://doi.org/10.1016/j.parint.2009.10.007>

891 Olstad, K., Bachmann, L., Bakke, T. a, 2009. Phenotypic plasticity of taxonomic and diagnostic

892 structures in gyrodactylosis-causing flatworms (Monogenea, Platyhelminthes). Parasitology
893 136, 1305–1315. <https://doi.org/10.1017/S0031182009990680>

894 Ondračková, M., Matějusková, I., Grabowska, J., 2012. Introduction of *Gyrodactylus perccotti*
895 (Monogenea) into Europe on its invasive fish host, Amur sleeper (*Perccottus glenii*, Dybowski
896 1877). Helminthologia 49, 21–26. <https://doi.org/10.2478/s11687-012-0004-3>

897 Pariselle, A., Boeger, W.A., Snoeks, J., Bilong Bilong, C.F., Morand, S., Vanhove, M.P.M., 2011. The
898 monogenean parasite fauna of cichlids: a potential tool for host biogeography. Int. J. Evol.
899 Biol. 2011, 471480, 10.4061/2011/471480. <https://doi.org/10.4061/2011/471480>

900 Pariselle, A., Muterezi Bukinga, F., Van Steenberge, M., Vanhove, M.P.M., 2015. Ancyrocephalidae
901 (Monogenea) of Lake Tanganyika: IV: *Cichlidogyrus* parasitizing species of Bathybatini
902 (Teleostei, Cichlidae): reduced host-specificity in the deepwater realm? Hydrobiologia 748,
903 99–119. <https://doi.org/10.1007/s10750-014-1975-5>

904 Pettersen, R.A., Mo, T.A., Hansen, H., Vøllestad, L.A., 2015. Genetic population structure of
905 *Gyrodactylus thymalli* (Monogenea) in a large Norwegian river system. Parasitology 142,
906 1693–1702. <https://doi.org/10.1017/S003118201500133X>

907 Phiri, H., Shirakihara, K., 1999. Distribution and seasonal movement of pelagic fish in southern
908 Lake Tanganyika. Fish. Res. 41, 63–71. [https://doi.org/10.1016/S0165-7836\(99\)00008-9](https://doi.org/10.1016/S0165-7836(99)00008-9)

909 Plisnier, P.-D., Chitamwebwa, D., Mwape, L., Tshibangu, K., Langenberg, V., Coenen, E., 1999.
910 Limnological annual cycle inferred from physical-chemical fluctuations at three stations of
911 Lake Tanganyika, in: Lindqvist, O.V., Mölsä, H., Salonen, K., Sarvala, J. (Eds.), From Limnology
912 to Fisheries: Lake Tanganyika and Other Large Lakes. Springer Netherlands, Dordrecht, pp.
913 45–58. https://doi.org/10.1007/978-94-017-1622-2_4

914 Plisnier, P.D., Mgana, H., Kimirei, I., Chande, A., Makasa, L., Chimanga, J., Zulu, F., Cocquyt, C.,

915 Horion, S., Bergamino, N., Naithani, J., Deleersnijder, E., André, L., Descy, J.P., Cornet, Y.,
916 2009. Limnological variability and pelagic fish abundance (*Stolothrissa tanganicae* and *Lates*
917 *stappersii*) in Lake Tanganyika. *Hydrobiologia* 625, 117–134. [https://doi.org/10.1007/s10750-](https://doi.org/10.1007/s10750-009-9701-4)
918 009-9701-4

919 Podsetchine, V., Huttula, T., 2000. Numerical simulation of wind-driven circulation in lake
920 tanganyika. *Aquat. Ecosyst. Heal. Manag.* 3, 55–64.
921 <https://doi.org/10.1080/14634980008656991>

922 Poulin, R., 2007. *Evolutionary ecology of parasites*. 2nd ed. Princeton University Press, Princeton,
923 New Jersey.

924 R Core Team, 2013. *R: A language and environment for statistical computing*. R Foundation for
925 Statistical Computing, Vienna, Austria.

926 Rambaut, A., Drummond, A.J., Xie, D., Baele, G., Suchard, M.A., 2018. Posterior summarization in
927 Bayesian phylogenetics using Tracer 1.7. *Syst. Biol* 67, 2.
928 <https://doi.org/10.1093/sysbio/syy032>

929 Řehulková, E., Mendlová, M., Šimková, A., 2013. Two new species of *Cichlidogyrus* (Monogenea:
930 Dactylogyridae) parasitizing the gills of African cichlid fishes (Perciformes) from Senegal:
931 Morphometric and molecular characterization. *Parasitol. Res.* 112, 1399–1410.
932 <https://doi.org/10.1007/s00436-013-3291-9>

933 Rieseberg, L.H., Kim, S.-C., Randell, R.A., Whitney, K.D., Gross, B.L., Lexer, C., Clay, K., 2007.
934 Hybridization and the colonization of novel habitats by annual sunflowers. *Genetica* 129,
935 149–165. <https://doi.org/10.1007/s10709-006-9011-y>

936 Rodríguez-González, A., Míguez-Lozano, R., Llopis-Belenguer, C., Balbuena, J.A., 2015. Phenotypic
937 plasticity in haptor structures of *Ligophorus cephalis* (Monogenea: Dactylogyridae) on the

938 flathead mullet (*Mugil cephalus*): a geometric morphometric approach. *Int. J. Parasitol.* 45,
939 295–303. <https://doi.org/10.1016/j.ijpara.2015.01.005>

940 Rohlf, F., 2006. Tpsdig, digitize landmarks and outlines. Version 2.10. Stony Brook, NY: State
941 University.

942 Rohlf, F.J., 1993. Relative warp analysis and an example of its application to mosquito wings, in:
943 Marcus, L., Bello, E., Garcia-Valdecasas, A. (Eds.), *Contributions to Morphometrics*. Stony
944 Brook, NY: State University, New York, pp. 132–158.

945 Sako, A., O'Reilly, C.M., Hannigan, R., Bickford, N., Johnson, R.L., 2005. Variations in otolith
946 elemental compositions of two clupeid species, *Stolothrissa tanganicae* and *Limnothrissa*
947 *miodon* in Lake Tanganyika. *Geochemistry Explor. Environ. Anal.* 5, 91–97.
948 <https://doi.org/10.1144/1467-7873/03-039>

949 Schelkle, B., Faria, P.J., Johnson, M.B., van Oosterhout, C., Cable, J., 2012. Mixed infections and
950 hybridisation in monogenean parasites. *PLoS One* 7, e39506.
951 <https://doi.org/10.1371/journal.pone.0039506>

952 Scott, M.E., Nokes, D.J., 1984. Temperature-dependent reproduction and survival of *Gyrodactylus*
953 *bullatarudis* (Monogenea) on guppies (*Poecilia reticulata*). *Parasitology* 89, 221–228.
954 <https://doi.org/10.1017/S0031182000001256>

955 Sefc, K., Mattersdorfe, K., Ziegelbecker, A., Neuhüttler, N., Steiner, O., Goessler, W., Koblmüller, S.,
956 2017. Shifting barriers and phenotypic diversification by hybridization. *Ecol. Lett.* 20, 651–
957 662.

958 Seixas, F.A., Boursot, P., Melo-Ferreira, J., 2018. The genomic impact of historical hybridization
959 with massive mitochondrial DNA introgression. *Genome Biol.* 19, 91.
960 <https://doi.org/10.1186/s13059-018-1471-8>

961 Shaw, P.W., Turner, G.F., Iddid, M.R., Robinson, R.L., Carvalho, G.R., 2000. Genetic population
962 structure indicates sympatric speciation of Lake Malawi pelagic cichlids. Proc. R. Soc. B Biol.
963 Sci. 267, 2273–2280. <https://doi.org/10.1098/rspb.2000.1279>

964 Shi, S.-F., Li, M., Yan, S., Wang, M., Yang, C.-P., Lun, Z.-R., Brown, C.L., Yang, T.-B., 2014.
965 Phylogeography and demographic history of *Gotocotyla sawara* (Monogenea: Gotocotylidae)
966 on Japanese Spanish mackerel (*Scomberomorus niphonius*) along the coast of China. J.
967 Parasitol. 100, 85–92. <https://doi.org/10.1645/13-235.1>

968 Strona, G., 2015. The underrated importance of predation in transmission ecology of direct
969 lifecycle parasites. Oikos 124, 685–690. <https://doi.org/doi:10.1111/oik.01850>

970 Sturmbauer, C., Baric, S., Salzburger, W., Rüber, L., Verheyen, E., 2001. Lake level fluctuations
971 synchronize genetic divergences of cichlid fishes in African lakes. Mol. Biol. Evol 18, 144–154.

972 Sturmbauer, C., Börger, C., Van Steenberge, M., Koblmüller, S., 2017. A separate lowstand lake at
973 the northern edge of Lake Tanganyika? Evidence from phylogeographic patterns in the cichlid
974 genus *Tropheus*. Hydrobiologia 791, 51–68. <https://doi.org/10.1007/s10750-016-2939-8>

975 Suchard, M.A., Lemey, P., Baele, G., Ayres, D.L., Drummond, A.J., Rambaut, A., 2018. Bayesian
976 phylogenetic and phylodynamic data integration using BEAST 1.10. Virus Evol. 4.
977 <https://doi.org/10.1093/ve/vey016>

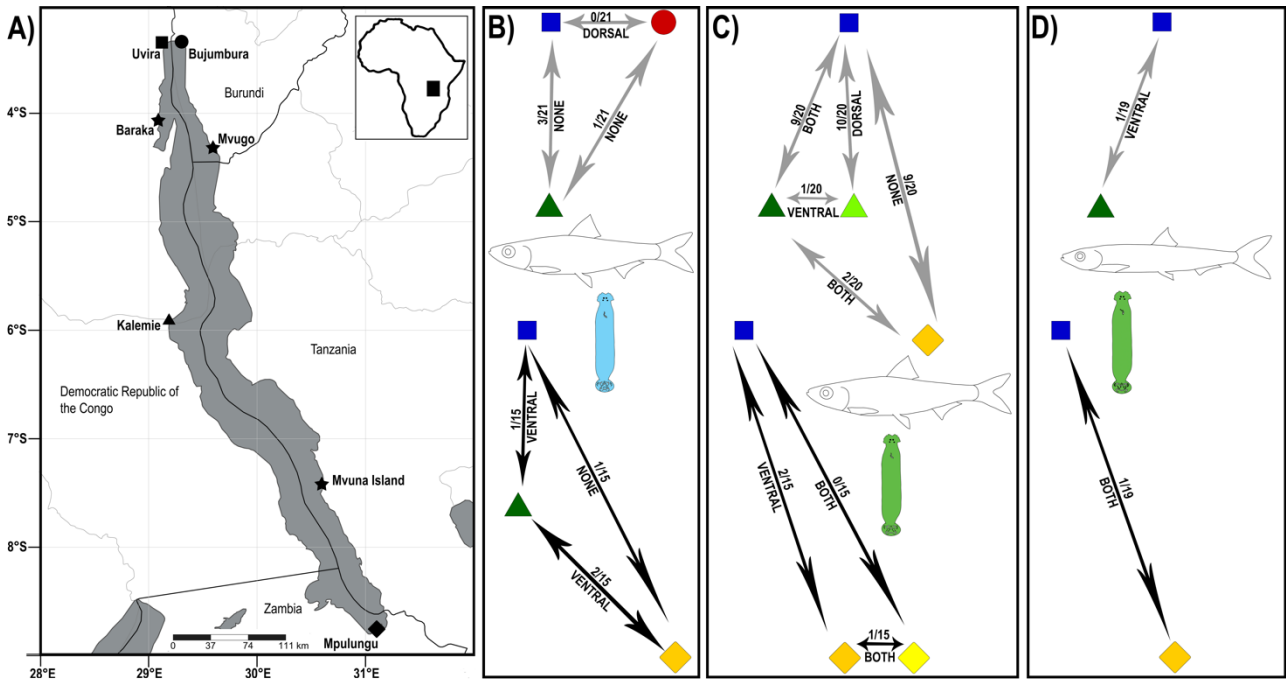
978 Svedäng, H., André, C., Jonsson, P., Elfman, M., Limburg, K.E., 2010. Migratory behaviour and
979 otolith chemistry suggest fine-scale sub-population structure within a genetically
980 homogenous Atlantic Cod population. Environ. Biol. Fishes 89, 383–397.
981 <https://doi.org/10.1007/s10641-010-9669-y>

982 Tajima, F., 1989. Statistical methods to test for nucleotide mutation hypothesis by DNA
983 polymorphism. Genetics 123, 585–595. <https://doi.org/PMC1203831>

- 984 Tinsley, R.C., 2004. Platyhelminth parasite reproduction: some general principles derived from
985 monogeneans. *Can. J. Zool.* 82, 270–291. <https://doi.org/10.1139/z03-218>
- 986 van Zwieten, P.A.M., Roest, F.C., Machiels, M.A.M., van Densen, W.L.T., 2002. Effects of inter-
987 annual variability, seasonality and persistence on the perception of long-term trends in catch
988 rates of the industrial pelagic purse-seine fishery of northern Lake Tanganyika (Burundi). *Fish.*
989 *Res.* 54, 329–348. [https://doi.org/10.1016/S0165-7836\(01\)00267-3](https://doi.org/10.1016/S0165-7836(01)00267-3)
- 990 Vignon, M., Pariselle, A., Vanhove, M.P.M., 2011. Modularity in attachment organs of African
991 *Cichlidogyrus* (Platyhelminthes: Monogenea: Ancyrocephalidae) reflects phylogeny rather
992 than host specificity or geographic distribution. *Biol. J. Linn. Soc.* 102, 694–706.
993 <https://doi.org/10.1111/j.1095-8312.2010.01607.x>
- 994 Vilas, R., Criscione, C.D., Blouin, M.S., 2005. A comparison between mitochondrial DNA and the
995 ribosomal internal transcribed regions in prospecting for cryptic species of platyhelminth
996 parasites. *Parasitology* 131, 839. <https://doi.org/10.1017/S0031182005008437>
- 997 Wang, M., Yan, S., Brown, C.L., Shaharom-harrison, F., Shi, S., Yang, T., 2016. Phylogeography of
998 *Tetrancistrum nebulosi* (Monogenea, Dactylogyridae) on the host of mottled spinefoot
999 (*Siganus fuscescens*) in the South China Sea, inferred from mitochondrial COI and ND2 genes.
1000 *Mitochondrial DNA* 27, 3865–3875. <https://doi.org/10.3109/19401736.2014.971240>
- 1001 Watanabe, Y., Zenitani, H., Kimura, R., 1995. Population decline off the Japanese sardine *Sardinops*
1002 *melanostictus* owing to recruitment failures. *Can. J. Fish. Aquat. Sci.* 52, 1609–1616.
1003 <https://doi.org/10.1139/f95-154>
- 1004 Wickham, H., 2009. Introduction, in: *Ggplot2*. Springer New York, New York, NY, pp. 1–7.
1005 https://doi.org/10.1007/978-0-387-98141-3_1
- 1006 Xiaojin, X., Weijun, W., Weijian, Y., 2000. The life span of *Dactylogyrus vaginulatus* on

- 1007 *Hypophthalmichthys molitrix*. Journal Nanjing Agric. Univ. 22, 95–98.
- 1008 Yan, S., Wang, M., Yang, C.-P., Zhi, T.-T., Brown, C.L., Yang, T.-B., 2016. Comparative
1009 phylogeography of two monogenean species (Mazocraeidae) on the host of chub mackerel,
1010 *Scomber japonicus*, along the coast of China. Parasitology 143, 594–605.
1011 <https://doi.org/10.1017/S0031182016000160>
- 1012 Zelditch, M., Swiderski, D.L., Sheets, H.D., 2012. Geometric morphometrics for biologists : a
1013 primer. Elsevier, London.
- 1014
- 1015

1016 **Figure captions**



1017

1018 **Fig. 1: Sampling sites in Lake Tanganyika with an overview of significant results of morphometric**

1019 **(above arrow) and geomorphometrics (below arrow) analyses between the specimens of**

1020 ***Kapentagyrys* spp. from the respective sampling sites. A) *K. limnotrissae*, B) *K. tanganicus* ex *L.***

1021 ***miodon* and C) *K. tanganicus* ex *S. tanganicae*. The morphometric results are presented as the**

1022 **number of variables which differ between the respective sampling sites (before the dash) vs the**

1023 **total number of variables analysed (after the dash). In the case of geomorphometrics, the**

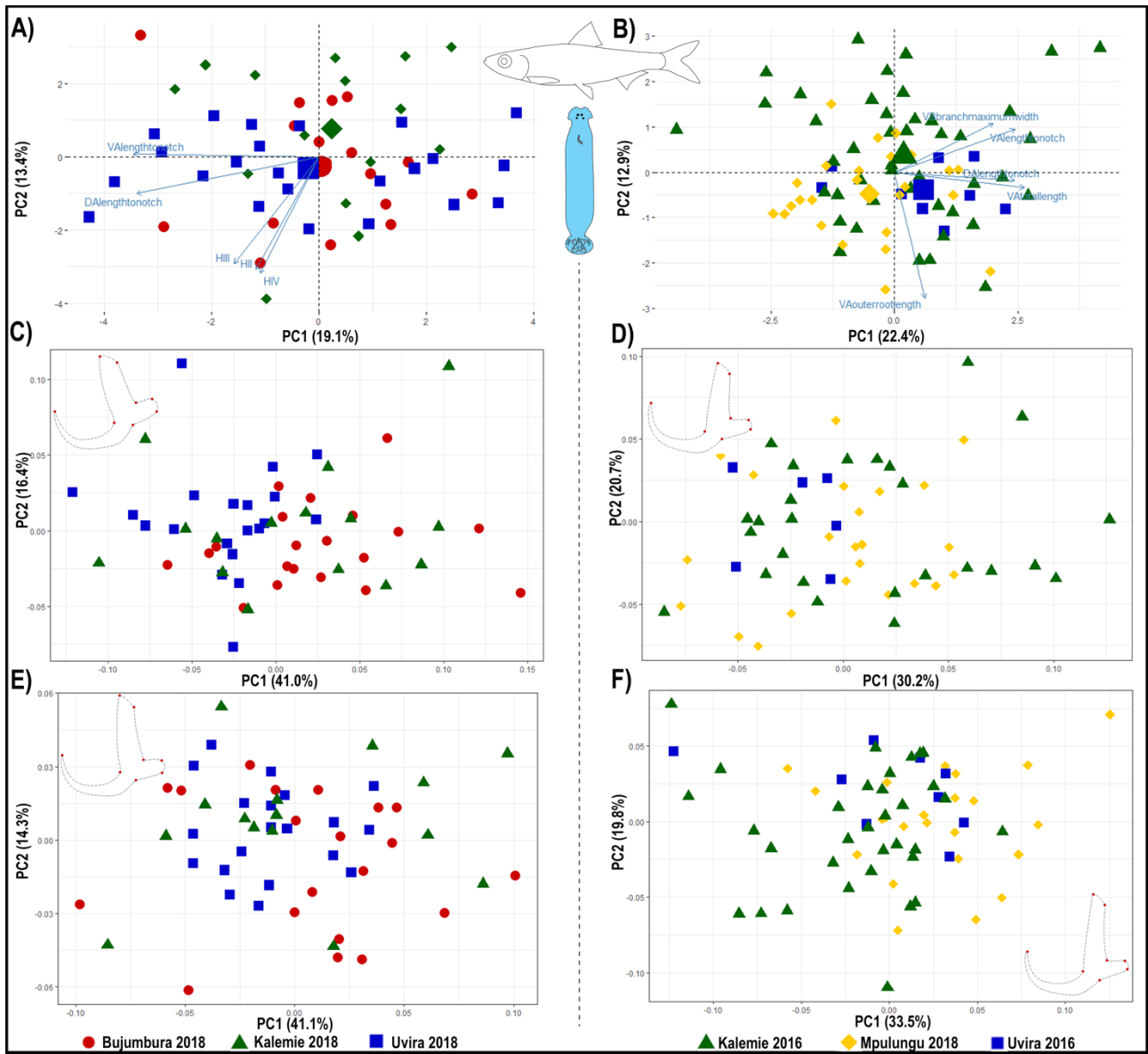
1024 **difference in either ventral, dorsal, both or none of the anchors is indicated. Shapes of signs**

1025 **correspond with the sampling site origin of specimens in the respective analyses. Colours of**

1026 **arrows refer to the separation on spatial (grey – ethanol preserved specimens) and spatio-**

1027 **temporal (black – fresh specimens) datasets. Map created using SimpleMappr software v7.0.0.**

1028 **(available at <http://www.simplemappr.net>. Accessed January 20, 2019).**



1029

1030

1031

1032

1033

1034

1035

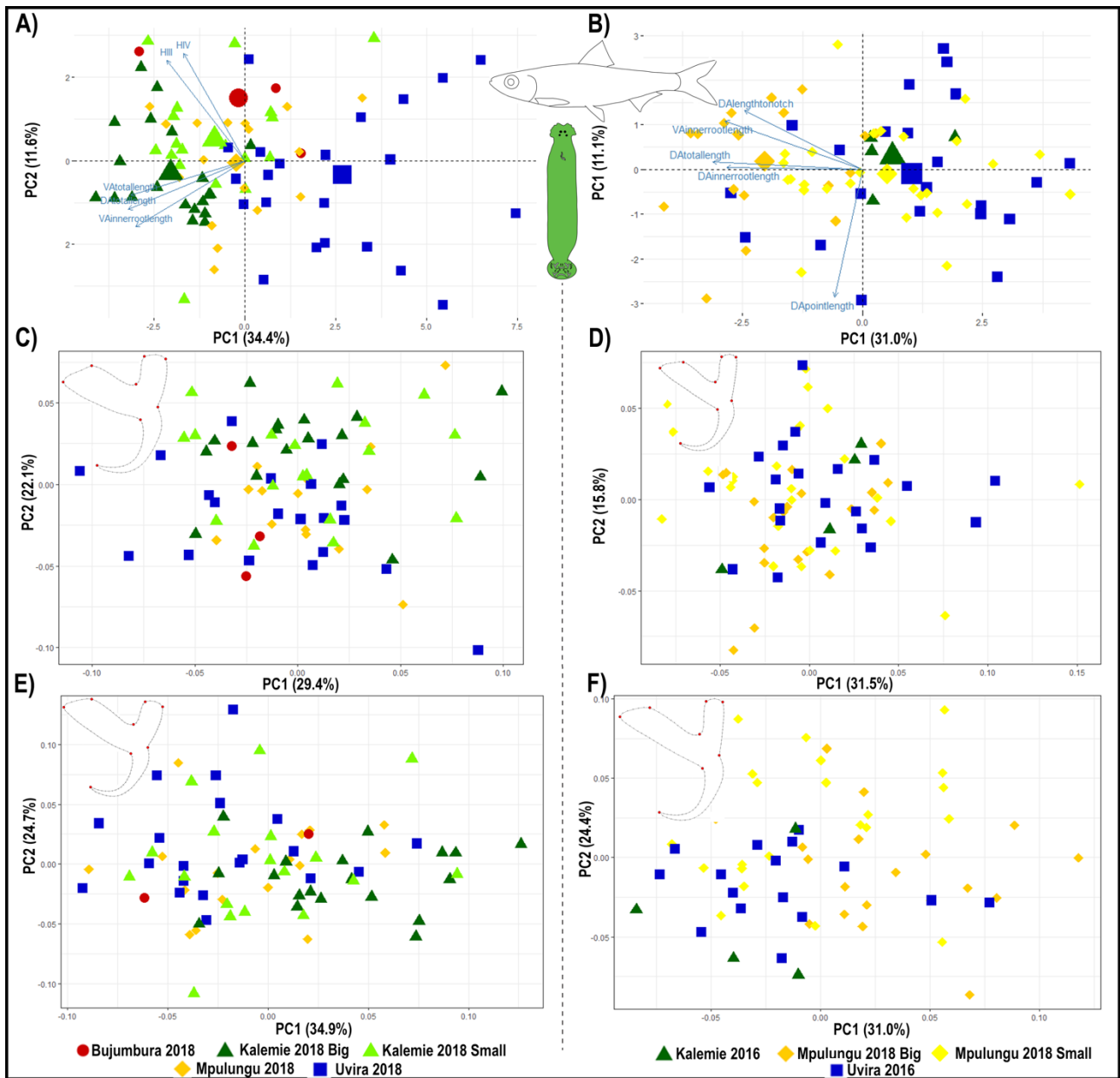
1036

1037

1038

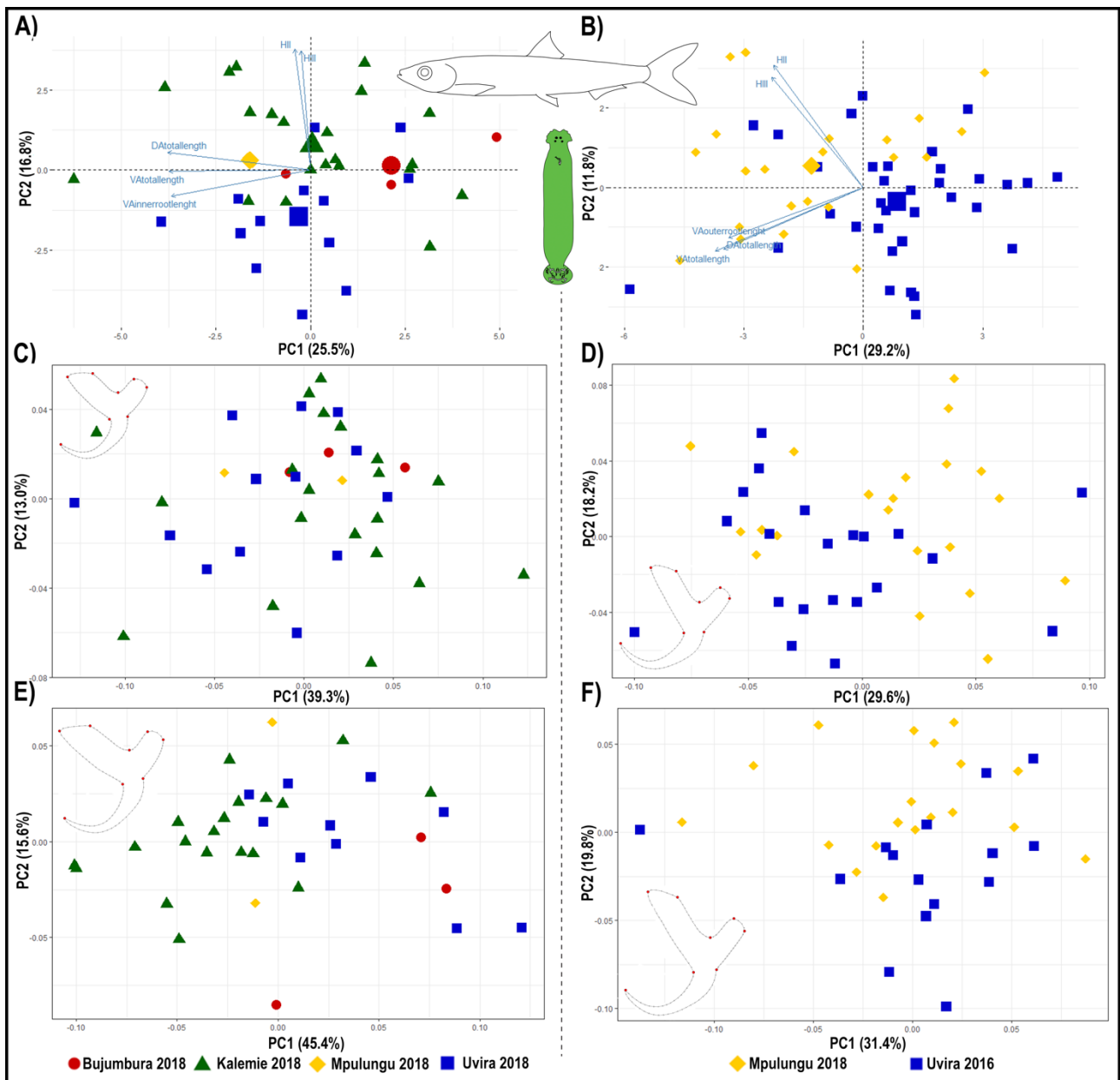
Fig. 2: Biplots showing the variation in haptoral structures of *K. limnotrissae*. Only the first two axes are shown. A) PCA of haptoral measurements with the five most contributing variables indicated by arrows, ethanol-preserved specimens (fifth and seventh pair of marginal hooks excluded due to missing data, the average position for each group is indicated by a larger size of the symbol); B) PCA of haptoral measurements with the five most contributing variables indicated by arrows, fresh specimens (second to seventh pair of marginal hooks excluded due to missing data, the average position for each group is indicated by a larger size of the symbol); C) PCA based on Procrustes distances of eight fixed landmarks describing the shape of the dorsal anchor, ethanol preserved specimens; D) PCA based on Procrustes distances of eight fixed landmarks

1039 describing the shape of the dorsal anchor, fresh specimens; E) PCA based on Procrustes distances
 1040 of eight fixed landmarks describing the shape of the ventral anchor, ethanol preserved specimens;
 1041 F) PCA based on Procrustes distances of eight fixed landmarks describing the shape of the ventral
 1042 anchor, ethanol preserved specimens. Consensus anchor shape for the respective analysis is
 1043 shown.



1044
 1045 **Fig. 3: Biplots showing the variation in haptoral structures of *K. tanganicanus* collected from *L.***
 1046 ***miodon* in this study. Only the first two axes are shown. A) PCA of haptoral measurements with**
 1047 **the five most contributing variables indicated by arrows, ethanol-preserved specimens (fifth to**

1048 seventh pair of marginal hooks excluded due to missing data, the average position for each group,
1049 is indicated by a larger size of the symbol); B) PCA of haptoral measurements with the five most
1050 contributing variables indicated by arrows, fresh specimens (second to seventh pair of marginal
1051 hooks excluded due to missing data, the average position for each group is indicated by a larger
1052 size of the symbol); C) PCA based on Procrustes distances of eight fixed landmarks describing the
1053 shape of the dorsal anchor, ethanol preserved specimens; D) PCA based on Procrustes distances of
1054 eight fixed landmarks describing the shape of the dorsal anchor, fresh specimens; E) PCA based on
1055 Procrustes distances of eight fixed landmarks describing the shape of the ventral anchor, ethanol
1056 preserved specimens; F) PCA based on Procrustes distances of eight fixed landmarks describing
1057 the shape of the ventral anchor, ethanol preserved specimens. Consensus anchor shape for the
1058 respective analysis is shown.



1059

1060

1061

1062

1063

1064

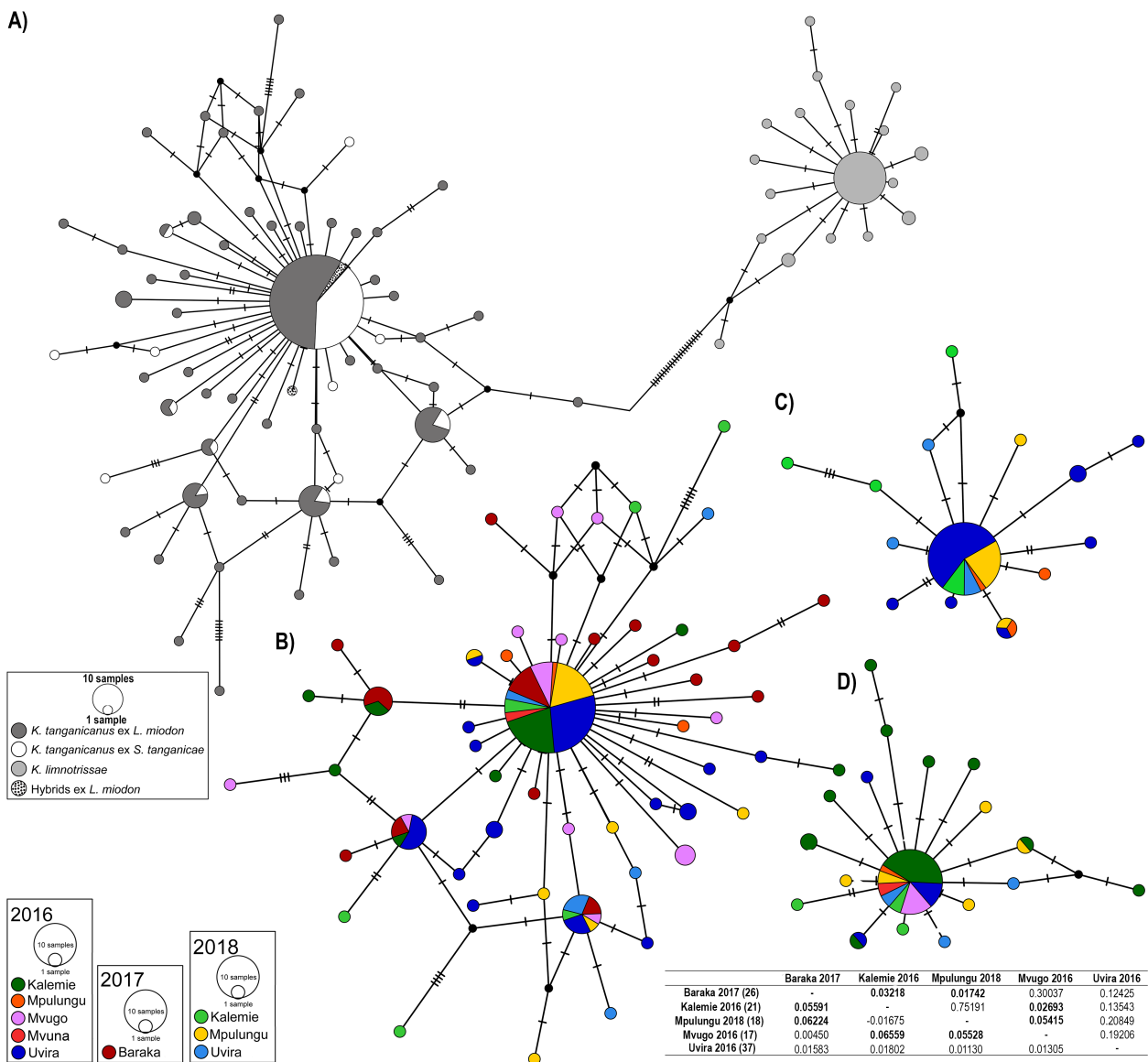
1065

1066

1067

Fig. 4: Biplots showing the variation in haptoral structures of *K. tanganicus* collected from *S. tanganicae* in this study. Only the first two axes are shown. A) PCA of haptoral measurements with the five most contributing variables indicated by arrows, ethanol-preserved specimens (fifth and seventh pair of marginal hooks excluded due to missing data, the average position for each group is indicated by a larger size of the symbol); B) PCA of haptoral measurements with the five most contributing variables indicated by arrows, fresh specimens (sixth and seventh pair of marginal hooks excluded due to missing data, the average position for each group is indicated by a larger size of the symbol); C) PCA based on Procrustes distances of eight fixed landmarks

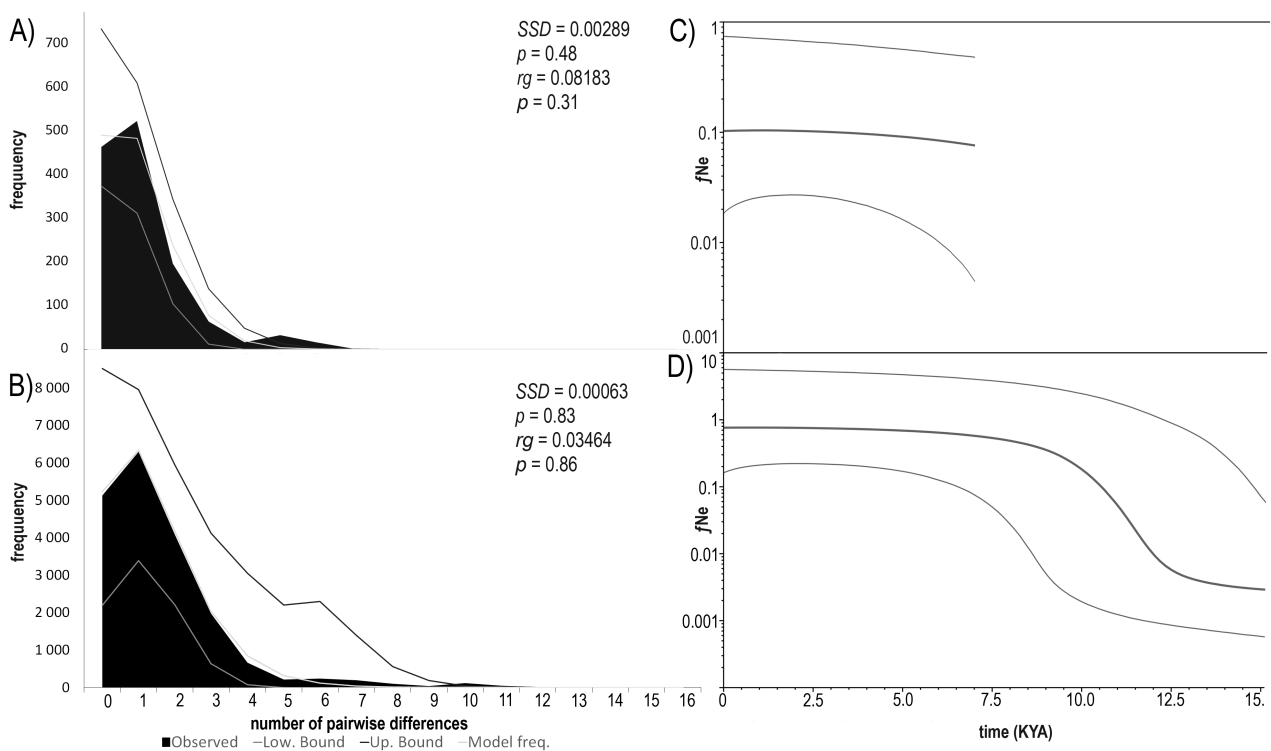
1068 describing the shape of the dorsal anchor, ethanol preserved specimens; D) PCA based on
 1069 Procrustes distances of eight fixed landmarks describing the shape of the dorsal anchor, fresh
 1070 specimens; E) PCA based on Procrustes distances of eight fixed landmarks describing the shape of
 1071 the ventral anchor, ethanol preserved specimens; F) PCA based on Procrustes distances of eight
 1072 fixed landmarks describing the shape of the ventral anchor, ethanol preserved specimens.
 1073 Consensus anchor shape for the respective analysis is shown.



1074
 1075 **Fig. 5: Genetic population structure of *Kapentagyris* spp. based on COI sequences (415 bp).**

1076 Median joining haplotype network of A) *K. tanganicanus* and *K. limnotrissae* with hybrid
 1077 individuals; B) *K. tanganicanus* ex *L. miodon*; C) *K. tanganicanus* ex *S. tanganicae*; D) *K.*

1078 *limnotrissae*. The circles represent different haplotypes with their size proportional to the number
 1079 of individuals represented. Haplotypes are connected with lines, indicating the number of
 1080 mutations. Small black circles indicate hypothetical haplotypes, predicted by the model. Colours
 1081 represent sampling events and host species, respectively, as mentioned in the legends. Genetic
 1082 differentiation among geographically pre-defined subpopulations of *K. tanganicus* ex *L. miodon*
 1083 listed in the enclosed table. Pairwise F_{ST} values and corresponding P-values are shown below and
 1084 above the diagonal, respectively. Significant results with $\alpha=0.05$ are marked in bold. Number of
 1085 monogean individuals in brackets.



1086

1087 **Fig. 6: Demographic history of *Kapentagyrus* spp.** Mismatch distribution for A) *K. limnotrissae* and
 1088 B) *K. tanganicus*. The black bars show the observed frequency of pairwise differences. The grey
 1089 lines refer to the expected distribution based on parameter estimates (plus 95% confidence limits)
 1090 under a model of population growth. The sum of squared differences (SSD) and the raggedness
 1091 index (rg) and their respective p-values are given to describe the fit of the observed distribution to
 1092 the expectations based on growth parameter estimates, as well as τ , the modal value of the

1093 mismatch distribution. Bayesian Skyline plot (BSP) of C) *K. limnotrissae* based on 415 base pairs of
1094 COI sequences and D) *K. tanganicus* based on 415 base pairs of COI sequences. BSPs show the
1095 effective populations size through time, assuming a substitution rate of 10% per site per million
1096 years in *Kapentagyris* spp. The thick line represents the median values; the thin lines denote 95%
1097 highest posterior density (HPD) intervals. The y-axis represents the population size parameter
1098 (product of female effective population size, fN_e , and mutation rate, μ).

1099 Table 1: Number of fish specimens of (a) *Limnothrissa miodon* and (b) *Stolothrissa tanganicae* examined for monogenean parasites along with sampling
 1100 site, basin and infection parameters. Values for *Kapentagyris limnothrissae* and *Kapentagyris tanganicanus* are shown before and after the dash,
 1101 respectively).

Sampling site (geographic coordinates, date, year)	Locality – basins (Danley et al. 2012)	Number of fish specimens	Number of monogenean individuals	Prevalence (%)	Infection intensity	Abundance (range)	Number of COI haplotypes (Genbank a.n)	Number of microscopic slides (a.n. in HU)
(a) <i>Limnothrissa miodon</i>								
Baraka (4°05'S–29°06'E; 29.7.2017)	The northern basin	24	10/63	16.7/41.7	2.5/5.4	0.4 (0–4)/2.1 (0–15)	–/26 (MK598222–47)	–/–
Bujumbura (3°23'S– 29°22'E; 10.4.2018)	The northern basin	30	108/4	83/10	4.3/1.3	3.6 (0–17)/ 0.1 (0–2)	–/–	X.4.13–37/ XII.2.10–13
Kalemie (5°56'S–29°12'E; 12.8.2016)	The central basin	10	55/5	80/33	6.9/1.7	5.5 (0–15)/0.5(0–2)	23 (MK598078–100)/21 (MK598145–65)	XI.1.11–2.12/ XI.3.49–50, 4.01–2, 19–20
Kalemie (12.4.2018)	The central basin	20	24/204	25/70	4.8/14.6	1.2 (0–11)/ 10.2 (0–37)	4 (MK598125–28)/8 (MK598137–44)	X.3.45–4.12/ XI.4.21, XII.1.01–38
Mpulungu (8°46'S– 31°07'E; 19.8.2016)	The southern basin	2	1/3	50/50	1/3	0.5(0–1)/1.5(0–3)	1 (MK598114)/3 (MK598248–50)	XI.2.21–22/–
Mpulungu (7.4. – 21.4.2018)	The southern basin	81	60/452	28/63	2.6/9	0.7 (0–8)/ 5.6 (0–42)	6 (MK598115–20)/18 (MK598251–68)	X.3.26–44/ XI.4.22–50, XII.2.10–28
Mvugo (4°18'S–29°34'E. 4.8.2016)	The northern basin	6	9/25	50/100	3/4.2	1.5 (0–3)/4.2 (1–10)	2 (MK598112–13)/17 (MK598205-21)	XI.2.13–20/ XI.4.03–18
Mvuna Island (7°26'S– 30°36'E 1.4.2015)	The southern basin	6	11/5	50/50	3.7/1.7	1.8 (0–8)/0.8 (0–3)	5 (MK598101–5) /2 (MK59817–8)	XI.2.33–37/–
Uvira (3°22' S–29°08'E; 11.8.2016)	The northern basin	41	12/28	35/40	1.7/3.5	0.6 (0–3)/1.4(0–9)	6 (MK598106–11)/37 (MK598166–76, 79–204)	XI.1.11–20/ XI.3.26–48
Uvira (12.4.2018)	The northern basin	30	43/70	53/76.7	2.7/3.0	1.4 (0–7)/ 2.3 (0–8)	4 (MK598121-24)/8 (MK598129-36)	X.4.38–50, XI.1.01–10/ XII.1.39–2.09
(b) <i>Stolothrissa tanganicae</i>								
Bujumbura (10.4.2018)	The northern basin	30	5	16.7	1	0.17 (0–1)	–	XII.3.48–3.50
Kalemie (11.8.2016)	The central basin	33	0	0	0	0	–	-
Kalemie (12.4.2018)	The central basin	30	44	66.7	2.2	1.5 (0–5)	7 (MK598317–23)	XII.3.26–3.47
Mpulungu (19.8.2016)	The southern basin	18	3	16.7	1	0.17 (0–1)	3 (MK598269, 81–82)	XII.4.24–25
Mpulungu (7.4. – 21.4.2018)	The southern basin	84	107	52.4	2.4	1.3 (0–13)	11 (MK598270–80)	XII.3.15–3.25, 4.01–2

Uvira (11.8.2016)	The northern basin	27	31	44	2.6	1.1 (0–6)	29 (MK598283–311)	XII.2.38–3.10
Uvira (12.4.2018)	The northern basin	25	12	28	1.7	0.5 (0–3)	5 (MK598312–16)	XII.4.03–15

1102

1103 Table 2: Genetic diversity indices of species of *Kapentagyris*, and their hosts *Limnothrissa miodon* and *Stolothrissa tanganicae* (De Keyzer et al.,
1104 2019) inferred from the COI mtDNA region.

Species	N	H	S	Hd	π	Max. divergence (%)
<i>K. limnotrissae</i>	51	19	18	0.6329±0.0800	0.002241±0.001742	1.2
<i>K. tanganicanus</i>	195	60	68	0.7341±0.0348	0.003800±0.002515	3.1
<i>K. tanganicanus</i> ex <i>L. miodon</i>	140	53	64	0.8066±0.0339	0.004499±0.002869	3.1
<i>K. tanganicanus</i> ex <i>S. tanganicae</i>	55	14	17	0.4983±0.0838	0.001991±0.001604	1.4
<i>L. miodon</i>	69	38	45	0.9250±0.0236	0.008909±0.004799	3.2
<i>S. tanganicae</i>	96	46	48	0.8583±0.0337	0.003543±0.002174	1.2

1105 N sample size, H number of haplotypes, S number of polymorphic sites, Hd haplotype diversity, π nucleotide diversity.

1106